ATLAS Note

ATL-COM-PHYS-2016-485

Draft version 0.0

Search for Higgs pair production decaying to WW^*WW^* with two same-electric-charge leptons plus jets at ATLAS

Xinchou, Lou[a], Yaquan Fang[a], Weiming Yao[b], Liang Li[c], Xiaohu Sun[d], Shuyang Hu[c], Xingguo Li[c], Maosen Zhou[a]

[a] *Institute of High Energy Physics, Chinese Academy of Sciences*
[b] *Lawrence Berkeley National Laboratory and University of California, Berkeley*
[c] *Shanghai Jiao Tong University, China*
[d] *University of Alberta, Canada*
[e] *Shandong University, China*

19th February 2017

A search is performed for resonant and non-resonant Higgs pair production with each Higgs boson decaying to a W boson pair using $\boldsymbol{XXX}$ $\mathbf{fb^{-1}}$ of proton-proton collision data at $\sqrt{s}$ = 13 TeV recorded by the ATLAS detector at the Large Hadron Collider. The final state considered in this analysis contains two same-electric-charge leptons, missing energy and four jets. In this case, both electroweak and QCD backgrounds are strongly suppressed. The data are found to be consistent with the expectation of the backgrounds and an upper limit at 95% C.L. is set for the production cross section. For the non-resonant Higgs pair production, the observed (expected) upper limit on $\sigma(gg \rightarrow hh)$ is xxx pb (xxx pb). For resonant Higgs pair production, the observed (expected) upper limits range from xxx pb (xxx pb) to xxx pb (xxx pb) as a function of resonant mass assuming that the narrow-width approximation holds.

Contents

1 Introduction

A Higgs boson was discovered by the ATLAS and CMS collaborations [1, 2] in 2012 and has been subsequently studied by spin and coupling measurements, which have established that its properties are very similar to the ones of the SM Higgs boson. These measurements are based on Higgs production via gluon-fusion, vector-boson-fusion and in association with a W or Z boson. Higgs pair production has not been measured and, if its value is similar to the SM predicted value, it is impossible to measure with the current data. However, the Higgs pair production can be significantly enhanced either by altering the Higgs boson self-coupling λ_{HHH} or in extended Higgs sectors such as 2-Higgs-Doublet Model (2HDM). In RUN I, various channels were explored with the ATLAS detector, such as $bb\gamma\gamma$ [3], $bbbb$ [4], $bb\tau\tau$ and $WW\gamma\gamma$ [5]. $WWWW$ channel with two same sign leptons or three leptons have been studied phenomenologically [6, 7]. This note provides supporting material for the search of Higgs pair production with the decay of $hh \rightarrow WWWW$ where a pair of the same signed Ws decay to leptons and the rest to hadrons. The multi-lepton selection can strongly suppress the QCD backgrounds. In addition, the same sign lepton requirement can further reduce the standard model backgrounds, such as $t\bar{t}$, Drell-Yang, and W^+W^- processes. The analyses for different processes but with similar event signature have been studied by other groups at ATLAS, such as SUSY, $t\bar{t}h$, and the same sign W pair searches [8, 9].

This note is organized as follows. In Section 2, the current data and the MC samples relevant for this analysis are described. Section 3 defines the objects such as lepton, jet etc. used in this analysis. In Section 4.1 the pre event selections and signal topology are summarized. The estimations of the different backgrounds are discussed in section 5. After backgroud estimations, signal optimizations are performed in section 6. In section **??**, the systematic uncertainties are presented. The event yields of the searches for resonant and non-resonant higgs pair are addressed in sectoin **??**. Section 7 documents the statistical procedure used to extract the sensitivity of the analysis. Finally, section 8 summarizes the results and conclusions of the study in this note.

1.1 The ATLAS detector

The ATLAS detector [10] at the LHC covers nearly the entire solid angle around the collision point. It consists of an inner tracking detector surrounded by a thin superconducting solenoid, electromagnetic and hadronic calorimeters, and a muon spectrometer incorporating three large superconducting toroid magnets. The inner-detector system (ID) is immersed in a 2 T axial magnetic field and provides charged particle tracking in the range $|\eta| < 2.5$.

The high-granularity silicon pixel detector covers the vertex region and typically provides three measurements per track, the first hit being normally in the innermost layer. It is followed by the silicon microstrip tracker which usually provides four two-dimensional measurement points per track. These silicon detectors are complemented by the transition radiation tracker, which enables radially extended track reconstruction up to $|\eta| = 2.0$. The transition radiation tracker also provides electron identification information based on the fraction of hits (typically 30 in total) above a higher energy deposit threshold corresponding to transition radiation.

The calorimeter system covers the pseudorapidity range $|\eta| < 4.9$. Within the region $|\eta| < 3.2$, electromagnetic calorimetry is provided by barrel and endcap high-granularity lead/liquid-argon (LAr) electromagnetic calorimeters, with an additional thin LAr presampler covering $|\eta| < 1.8$, to correct for energy loss in material upstream of the calorimeters. Hadronic calorimetry is provided by the steel/scintillating-tile calorimeter, segmented into three barrel structures within $|\eta| < 1.7$, and two copper/LAr hadronic endcap calorimeters. The solid angle coverage is completed with forward copper/LAr and tungsten/LAr calorimeter modules optimised for electromagnetic and hadronic measurements respectively.

The muon spectrometer (MS) comprises separate trigger and high-precision tracking chambers measuring the deflection of muons in a magnetic field generated by superconducting air-core toroids. The precision chamber system covers the region $|\eta| < 2.7$ with three layers of monitored drift tubes, complemented by cathode strip chambers in the forward region, where the background is highest. The muon trigger system covers the range $|\eta| < 2.4$ with resistive plate chambers in the barrel, and thin gap chambers in the endcap regions. A three-level trigger system is used to select interesting events [11]. The Level-1 trigger is implemented in hardware and uses a subset of detector information to reduce the event rate to a design value of at most 75 kHz. This is followed by two software-based trigger levels which together reduce the event rate to about 200 Hz.

2 Data and Monte Carlo samples

2.1 Data samples

The data samples used in this analysis was recorded by ATLAS from D/M/Y to D/M/Y at $\sqrt{s} = 13$ TeV. And the data set must pass Good Run List, corresponding to a total integrated luminosity of xx fb^{-1}. The data set was produced with xAOD format, and followed HIGG8D1 derivation, which provides a reduction model specifically for the ttH analysis with multileptons in the final states. These reductions contain slimming(remove un-needed variables), thinning(remove entire objects from events) and skimming (remove whole event with very loose preselections). The skimming requires the event containing two good leptons that was only applied to datat, not to Monte Carlo samples yet. But in the future, the same skimming will apply to the Monte Carlo samples as well.

2.2 Monte Carlo samples

2.2.1 Signal samples

Signal samples were generated by MadGraph5 and Herwig++. For non-resonant signal, the event generation was performed using a next-to-leading order SM Higgs pair model [12] in MadGraph5. For resonant signal samples, the event generation was also performed using a next-to-leading order heavy resonant model [12] called $2HDMCP\_EFT$ in MadGraph5. The heavy scalar, H, is assumed to have narrow width with respect to the experimental resolution. The decay width of the H boson in the simulation is set to 10 MeV for the following mass points: 260 GeV, 300 GeV, 400 GeV and 500 GeV. The card used in MadGraph5 for signal event generations is attached in Appendix A. Subsequently, the H boson is required to decay into a pair of SM Higgs bosons, both of which decay into a pair of W bosons using Herwig++. Finally, two $W^+(W^-)$ are forced to decay leptonically (taus included), while the other two $W^-(W^+)$ hadronically. All the signal samples are list in Tab. 1. The cut flow for each mass point is presented in App. B. In the analysis, the two charge sides are considered simultaneously. The kinematic distributions of signal samples at preselection level are shown in Fig. 1. Besides basic transverse momentum of objects, many other plots of distributions of physical variables are made. The meanings of these variables are addressed

DSID	lepton charge	m_H [GeV]	Num. Events	Simulation	e/a/s/r/p-tags
344133	(+)	Non-res	500000	AFII	e5060, a766, a821, r7676, p2666
344134	(-)	Non-res	500000	AFII	e5060, a766, a821, r7676, p2666
343704	(+)	260	100000	AFII	e5234, a766, a821, r7676, p2719
343712	(-)	260	100000	AFII	e5234, a766, a821, r7676, p2719
343706	(+)	300	100000	AFII	e5234, a766, a821, r7676, p2719
343714	(-)	300	100000	AFII	e5234, a766, a821, r7676, p2719
343709	(+)	400	100000	AFII	e5153, a766, a821, r7676, p2719
343717	(-)	400	100000	AFII	e5153, a766, a821, r7676, p2719
343711	(+)	500	100000	AFII	e5153, a766, a821, r7676, p2719
343719	(-)	500	100000	AFII	e5234, a766, a821, r7676, p2719

Table 1: A list of the signal samples which have been produced for study.

in Sec. 4.1. For each kinematic variable, the events are split into three channels based on flavor of leptons, i.e. ee, $\mu\mu$ and $e\mu$. From these plots, no obvious differences of kinematic distributions can be spotted for different channels.

Apart from normalized distributions of signal samples, various comparisons between signal and all the backgrounds can be seen in Fig. 6 and Fig. 11, including prompt same-signed(promptSS) and data-driven backgrounds, which are explained in Sec. 2.2.2 and Sec. 5, respectively. For the purpose of a better view, the normalizations of signal distributions are rescaled to 1000(100) times as large as the luminosity used in this note, for ee($e\mu$, $e\mu$) channel.

	DSID	Process	Generator	cross-section(pb)	K-factor	Simulation
VV	361063	$llll$	Sherpa	12.583	0.91	Full
	361064	$lllvSFMinus$	Sherpa	1.8446	0.91	Full
	361065	$lllvOFMinus$	Sherpa	3.6235	0.91	Full
	361066	$lllvSFPlus$	Sherpa	2.5656	0.91	Full
	361067	$lllvOFPlus$	Sherpa	5.0169	0.91	Full
	361069	$llvvjj\_ss\_EW4$	Sherpa	0.02575	0.91	Full
	361070	$llvvjj\_ss\_EW6$	Sherpa	0.043375	0.91	Full
	361071	$lllvjj\_EW6$	Sherpa	0.042017	0.91	Full
	361072	$lllljj\_EW6$	Sherpa	0.1279	0.91	Full
	361073	$ggllll$	Sherpa	0.02095	0.91	Full
$t\bar{t}V$	410066	ttW_Np0	MadGraph+Pythia8	0.17656	1.32	Full
	410067	ttW_Np1	MadGraph+Pythia8	0.14062	1.32	Full
	410068	ttW_Np2	MadGraph+Pythia8	0.1368	1.32	Full
	410080	$4topSM$	MadGraph+Pythia8	0.0091622	1.0042	Full
	410081	$ttbarWW$	MadGraph+Pythia8	0.0080975	1.2231	Full
	410111	$ttee\_Np0$	MadGraph+Pythia8	0.0096235	1.51	Full
	410112	$ttee\_Np1$	MadGraph+Pythia8	0.017344	1.51	Full
	410113	$ttmumu\_Np0$	MadGraph+Pythia8	0.0096462	1.51	Full
	410114	$ttmumu\_Np1$	MadGraph+Pythia8	0.017361	1.51	Full
	410115	$tttautau\_Np0$	MadGraph+Pythia8	0.0098874	1.51	Full
	410116	$tttautau\_Np10$	MadGraph+Pythia8	0.01779	1.51	Full
tV	410013	$Wt\_inclusive\_top$	Powheg	34.009	1.054	Full
	410014	$Wt\_inclusive\_antitop$	Powheg	33.989	1.054	Full
	410049	$tZ\_4fl\_tchan\_trilepton$	Madgraph+Pythia	0.0090636	1.0	Full
	410215	$tWZDR$	Pythia8+EvtGen	0.015558	1.0	Full
$t\bar{t}H$	341177	$ttH \to ll + H$	aMC@NLO+Herwig++	0.05343	1.0	Full
	341270	$ttH \to ljets + H$	aMC@NLO+Herwig++	0.22276	1.0	Full
	341271	$ttH \to allhad + H$	aMC@NLO+Herwig++	0.23082	1.0	Full

Table 2: A list of the background samples that contribute two prompt same-signed leptons.

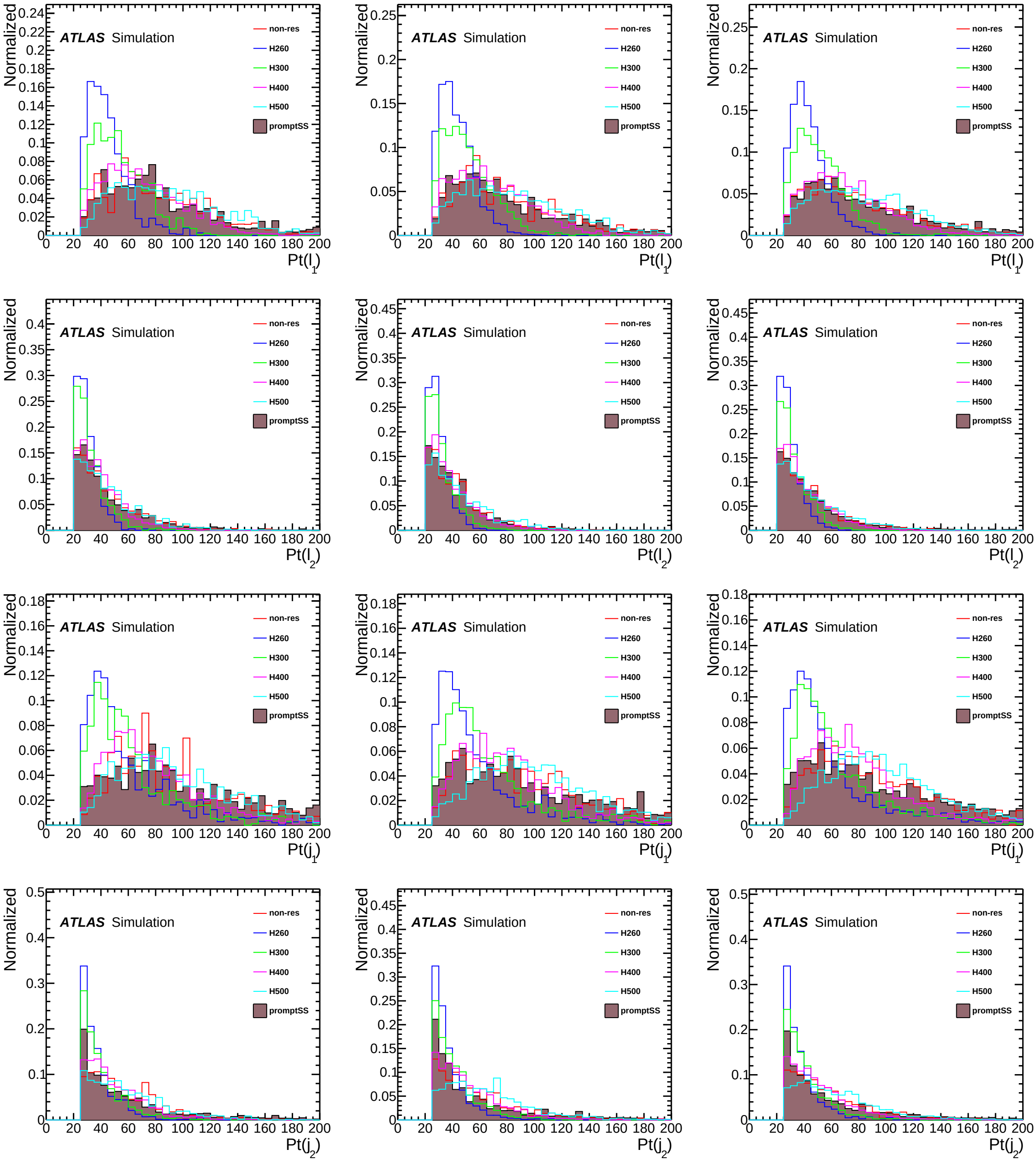
ATLAS Simulation
non-res
H260
H300
H400
H500
promptSS
Normalized
Pt(l1)
Pt(l2)
Pt(j1)
Pt(j2)

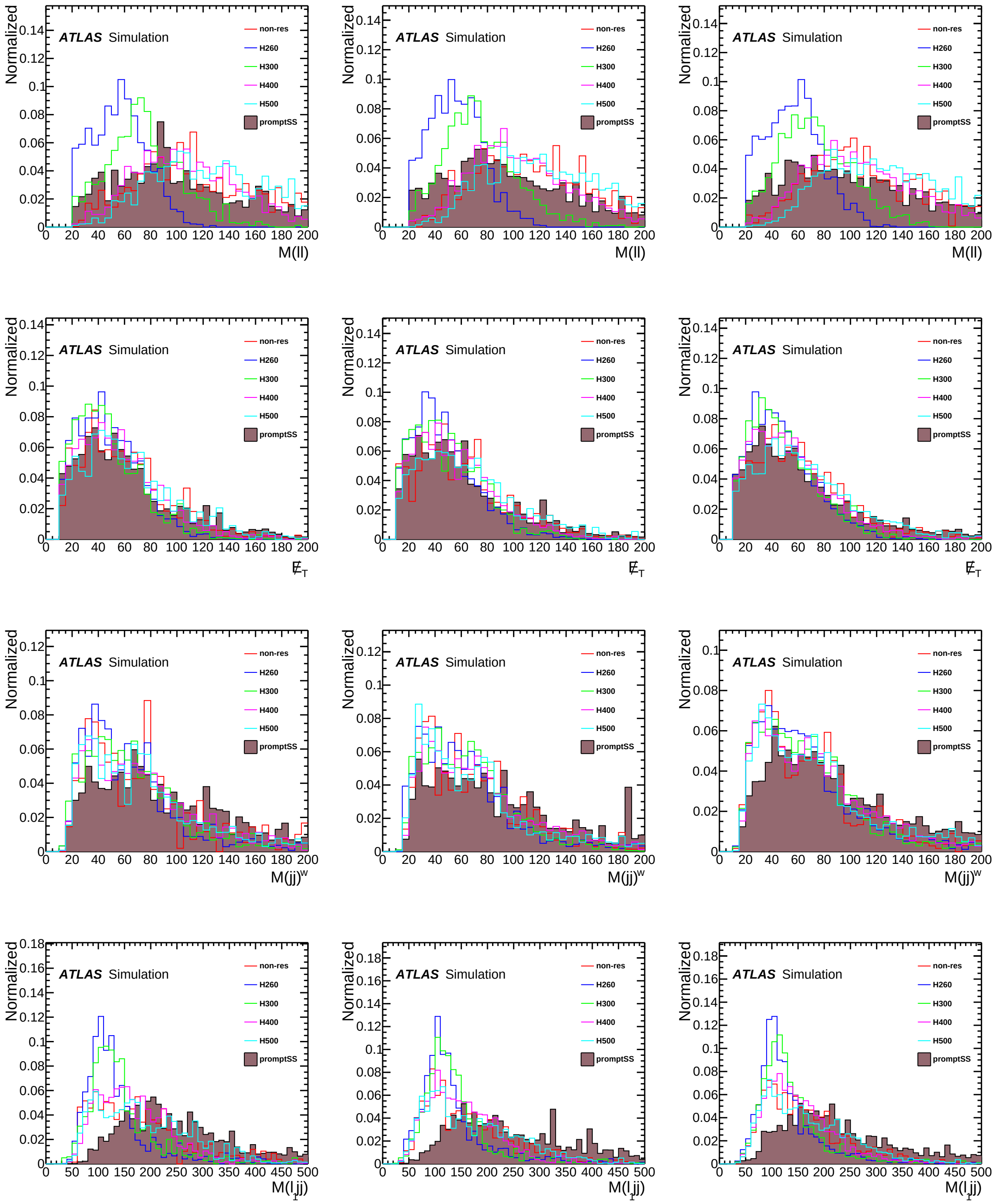
ATLAS Simulation
non-res
H260
H300
H400
H500
promptSS
Normalized
M(ll)
$\not{E}_T$
$M(jj)^W$
$M(l_1jj)$

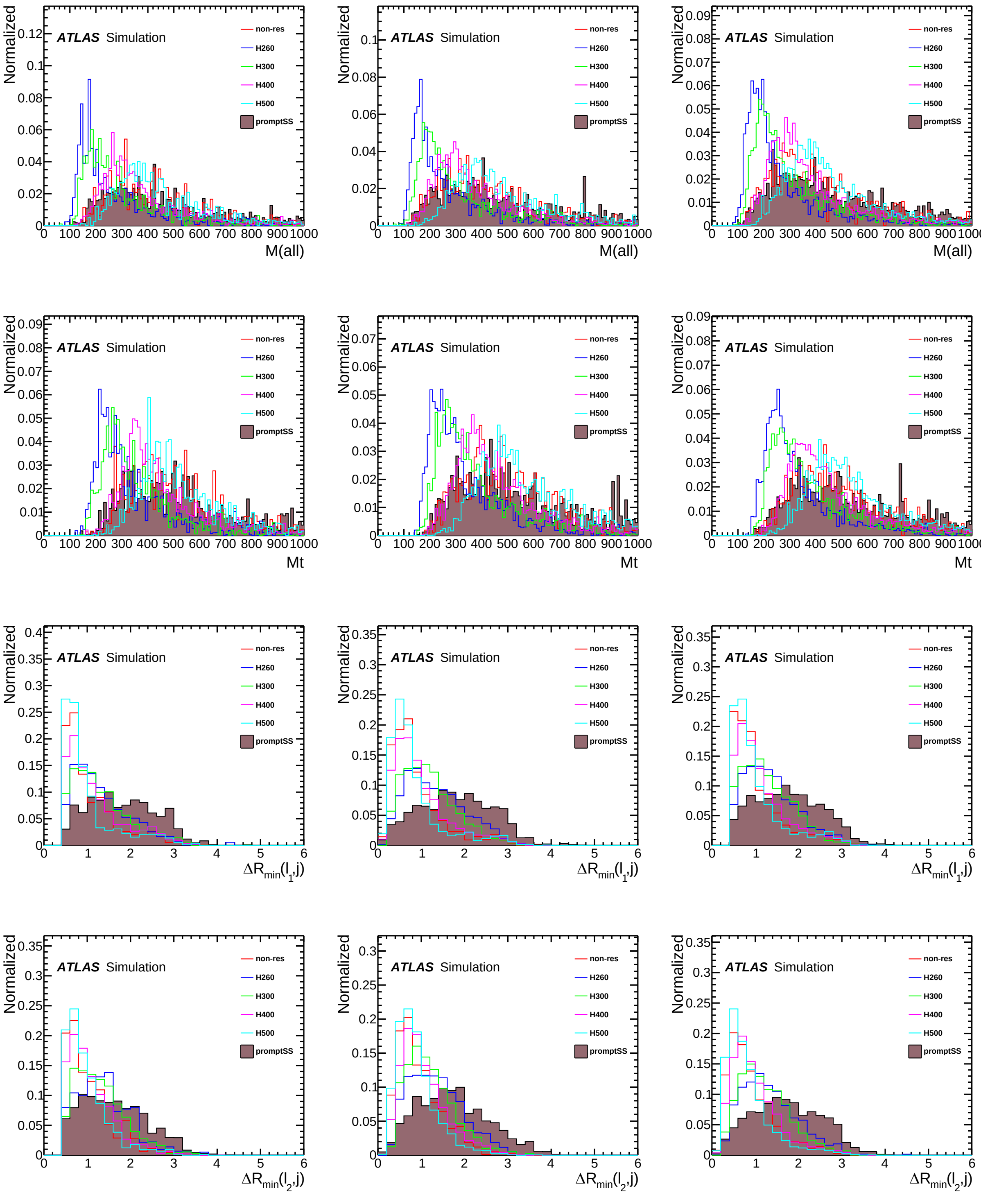

Figure 1: Kinematic distributions of signal and prompt same-signed backgrounds(promptSS)at pre-selection level. The promptSS are estimated from pure MC, including $t\bar{t}V$, VV, tV and $t\bar{t}H$. They contribute to promptSS according to individual cross-sections. Left: ee, middle: $\mu\mu$, right: $e\mu$. The meanings of kinematic variables are explained in Sec. 4.1.

2.2.2 Background samples

Diboson, Z+jet and W+jet events are generated with Sherpa v2.1. The CT10 PDF set is used for these samples. ttbar background events are generated with Powheg v2.0 and interfaced with Pythia6 for the parton showering and fragmentation. The Perugia 2012 (P2012) parameter set (tune) with the CTEQ6L PDF set is used for the underlying event (UE) description. A filter requiring at least one lepton is included. The $t\bar{t}$ cross section is 832 pb at $\sqrt{s}$ = 13 TeV. Powheg is also used to model other top backgrounds such as single top t-channel, s-channel and Wt. ttV background events are generated with MadGraph, interfaced with Pythia8 and A14 tune is used for showering. Three ttW background samples, plus 0, 1 and 2 partons are generated. The total ttW cross section is 566 fb at $\sqrt{s}$ = 13 TeV. The $ttZ(Z \to \ell\ell, \ell = e, \mu)$samples generated with 0 and 1 additional partons. Both on-shell and off-shell Z decays are included. The total ttZ cross section is 760fb at $\sqrt{s}$ = 13 TeV. All samples use NNPDF2.3LO PDF set. A list of background samples that contribute two same-signed leptons can be found in Tab. 2. More details can be found in this public note.

All Monte Carlo samples are processed through a detector simulation of the ATLAS detector response based on Geant4. Additional simulated pp collisions generated with Pythia8 were overlaid to model the effects of both in- and out-of-time pileup, from additional pp collisions in the same and nearby bunch crossings. The pileup distribution is reweighed to reflect the mean number of additional interactions observed in data. All simulated events were processed using the same reconstruction algorithms and analysis chain as the data. Simulated events are corrected so that the object reconstruction and identification efficiencies, energy scales and energy resolutions match those determined from data.

3 Object definition

The object definition is the same as ttH analysis, except that E_T^{miss} is added. We use the following criteria to select the leptons, jet, and missing E_T objects.

3.1 Electron

- p_T > 10 GeV
- $|\eta|$ <2.47, excluding $1.37 < |\eta| < 1.52$ to remove the crack.
- A likelihood-based discriminant is established based on shower shape variables in electromagnetic calorimeter and track qualities from inner detector. It is used to separate electrons from fakes mainly coming from hadron decays and photon conversion. The looseAndBLayer working point is used which gives approximate 95% electron efficiency.
- The working point of loose isolation is used.
- The longitudinal impact parameter of the electron track with respect to the selected event primary vertex, multiplied by the sine of the polar angle, $|z_0 sin\theta|$, is required to be less than 2 mm. The transverse impact parameter divided by the estimated uncertainty on its measurement, $d_0/\sigma(d_0)$, must be less than 10.

3.2 Muon

- $p_T > 10$ GeV.
- $|\eta| < 2.5$.
- Pass loose muon quality requirement.
- The working point of loose isolation is used.
- $|z_0 sin\theta| < 2$ mm, $d_0/\sigma(d_0) < 10$.

3.3 Jet

- "$anti - k_t$" algorithm with distance parameter R = 0.4 is used to reconstruct jets. Jets which come from beam background or fail in the regions with hot noisy calorimeter cells, are removed.
- $p_T > 25$ GeV
- $|\eta| < 2.5$
- To discriminate hard scattering jets from pile-up, jet with $p_T < 60$ GeV and $|\eta| < 2.4$ is required to satisfy the criteria based on a multivariate variable called the jet-vertex-tagger(JVT), which gives about 92% efficiency and about 2% fake rate.
- The MV2c10 algorithm is used to tag jets containing b-hadrons. This algorithm is based on the long lifetime, high decay multiplicity, hard fragmentation and high mass of b-hadrons. And a tight *b*-tagging working point is used that gives 70% efficiency to tag b-hadron jet.

3.4 Missing transverse energy

The missing transverse momentum, with magnitude E_T^{miss}, is calculated as the negative vectorial sum of the transverse momenta of all calibrated selected objects, such as electrons, muons, and jets. Tracks compatible with the primary vertex and not matched to any of those objects are also included in the reconstruction. This definition is called track soft term(TST)E_T^{miss}.

4 Event selection

4.1 Pre-selections

The events are required to pass the following pre-selection:

- **GRL**:XXX
- **event clean criteria**: cleaning for Tile corrupted events, LAr noise bursts and corrupted data.
- **trigger**: For 2015 data set, events are accepted passing any of following triggers:
  - HLT_mu20_iloose_L1MU15

  - HLT_mu50
  - HLT_e24_lhmedium_L1EM20VH
  - HLT_e60_lhmedium
  - HLT_e120_lhloose

  For 2016 data set: following triggers are used by "or" logic:

  - HLT_mu24_ivarmedium
  - HLT_mu50
  - HLT_e24_lhtight_nod0_ivarloose
  - HLT_e60_lhmedium_nod0
  - HLT_e140_lhloose_nod0

- **Object definitions**: select objects following Object definitions
- **Overlap removal**

Keep	Remove	Cone size $(\Delta R) or track)$
electron	tau	0.2
muon	tau	0.2
electron	CaloTagged muon	shared track
muon	electron	shared track
electron	jet	0.2
jet	electron	0.4
muon	jet	(0.2 or ghost-matched to muon) and numJetTrk≤2
jet	muon	0.4
tau	jet	0.2

Table 3: Table of overlap removal.

Pre-selection	GRL
	Event clean criteria
	Pass any trigger applied
	Select good objects
	Overlap removal
	Two tight same-signed leptons, with at least one trigger matched
	$Pt(\ell)^{matched} > 30$ GeV, $Pt(\ell_2) > 20$ GeV
	B veto
	$\not{E}_T$ >10 GeV
	$M(\ell\ell)$ >15 GeV
	$\lvert M(\ell\ell) - M(Z)\rvert$ >10 GeV in ee channel
	N_{jet} ≥2

Table 4: Summary of pre-selection.

To suppress fakes from background, tighter requirements are applied on lepton candidates. Any electron candidate has to pass the TightLH working point(WP) of likelihood based discriminant. Both E_T^{cone20}/pT and $p_T^{varcone20}/pT$ are required to be less than 0.06, which corresponds to the FixedCutTight isolation WP. For muon, Both Tight ID and FixedCutTightTrackOnly WP ($p_T^{varcone20}/pT < 0.06$) are required. The $|z_0 sin\theta|$ is less than 0.5 for both electron and muon candidates. And $|d_0/\sigma(d_0)|$ must be less than 3(5) for a muon(electron) candidate. there must be at least one lepton which matches any lepton trigger used. In addition, the trigger match is confirmed by that Pt of leading lepton being larger than 25 GeV. The Pt of sub leading lepton is required to be at least 20 GeV. This requirement on sub leading lepton is to suppress fakes(jet faking lepton). In order to suppress background from top quark associated processes, B veto is applied which means rejecting any events containing at least one B jet. And due to the fact that $Drell-Yan$ is not well modeled, the invariant mass of two tight leptons has to be larger than 20 GeV. And to suppress charge-mis-identification from Zjets, Z veo is applied for ee channel. Finally, for pre-selection level, the number of jets is required at least 2. All the pre-selections are summarized in Tab. 4.

In the analysis, events are split into three categories based on lepton favors: $e^\pm e^\pm$, $\mu^\pm\mu^\pm$, $e^\pm\mu^\pm$.

4.2 Control regions

At pre-selection level, two control regions are defined in Tab. 5, for $t\bar{t}$ and Zjets. Both $t\bar{t}$ and Zjets can contribute charge-mis-identification backgrounds in signal region. In addition, $t\bar{t}$ can be one source of jet

$t\bar{t}$	Two tight leptons with opposite sign leptons $(M(\ell\ell) - M(Z)) > 20$ GeV At least two b-jets
Zjets	Two tight leptons with opposite sign and same flavor $(M(\ell\ell) - M(Z)) < 45$ GeV B veto, at least one jet

Table 5: Definitions of $t\bar{t}$ and Z+jets control regions.

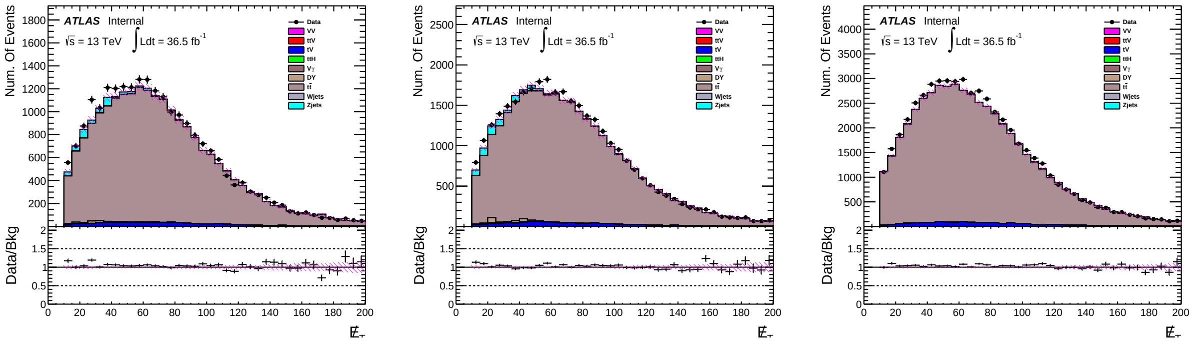

Figure 2: Distributions of missing transverse energy in the control region of $t\bar{t}$ sample. Left: ee, middle: $\mu\mu$, right: $e\mu$.

fakes. Although charge-mis-identification and jet fakes backgrounds are not going to be estimated using MC directly, both MC samples serve data-driven estimations, which will be explained later carefully. The kinematic distributions of $t\bar{t}$ and Zjets in each individual control region are shown in Fig. 2 and Fig. 3, respectively. They are dominant in each individual control region as expected, which confirms well modeling of $t\bar{t}$ and Zjets samples.

4.3 Signal topology

The signature of 2LSS is two same signed leptons plus jets. Initially, two SM higgs are probably in two opposite semi-sphere. Subsequently, both SM higgs decay to two W bosons, one of which is off-shell. The off-shell W will probably contribute quite soft jets. So, in this analysis, we divide the signal region to two categories based on number of jets. For 400 GeV, 500 GeV and non-res search, we require at least 3 jets; while for remaining mass points, i.e, 260 GeV and 300 GeV, at least 2 jets are required. And this has been checked with MC samples, each mass point does show the highest sensitivity in each individual category. The decay products of SM Higgs are close to each other in most cases, this signature can be extracted by kinematics: $\Delta R_{min}(\ell, j)$ and $M_{\ell_1 jj}$, which corresponds to ΔR distance between lepton and the closet jet, invariant mass of leading lepton and two closet jets, respectively. These kinematic variables are summarized below:

- $M(ll)$, the invariant mass of two same-signed leptons;
- $\not{E}_T$, missing transverse energy;
- $M(jj)^W$, the invariant mass of two closet jets among all selected good jets;
- $M(l_1jj)$, the invariant mass of leading lepton and two closet jets;

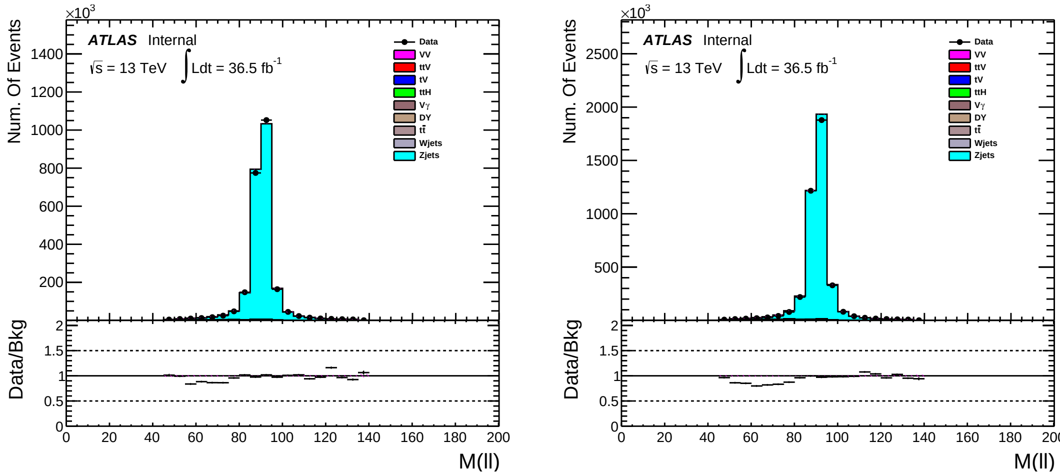

(a) (b)

Figure 3: Distributions of invariant mass of two tight leptons in the control region of Zjets sample. Left: ee, right: $\mu\mu$.

- $M(all)$, the invariant mass of all selected objects;
- Mt, the transverse mass of all selected objects;
- $\Delta R_{min}(\ell_1, j)$, ΔR distance between leading lepton and the closet jet;
- $\Delta R_{min}(\ell_2, j)$, ΔR distance between sub leading lepton and the closet jet;

All of their distributions can be found in Fig. 6 and Fig. 11.

5 Background estimation

There are several kinds of backgrounds: Prompt same-signed processes(promptSS), Charge-mis-identification (QmisID) and jet faking lepton(fakes). PromptSS are from those processes which contribute two prompt SS leptons, and are estimates with simulated samples. In this analysis, promptSS background consists of ttV, VV($W^{\pm}W^{\pm}$, WZ, ZZ), tV and ttH. QmisID is mainly from Z+jet and $t\bar{t}$(fully leptonic), in which one lepton is mis-identified with wrong charge. And jet fakes come from W+jet and $t\bar{t}$(semi-leptonic), in which one jet is mis-identified to lepton. The comparisons between pure MC and data are shown in Fig. 4. Large discrepancy can be see seen in three channels, which indicates the fact that QmisID and jet fakes are not well modeled with MC samples. So both QmisID and jet fakes are estimated with data-driven methods. In addition, there is small fraction of background that comes from $W\gamma$ process, where one photon is mis-identified as lepton. This will be estimated by simulated samples. Both data-driven methods will be performed at pre-selection level, because of enough statistics and systematics estimations.

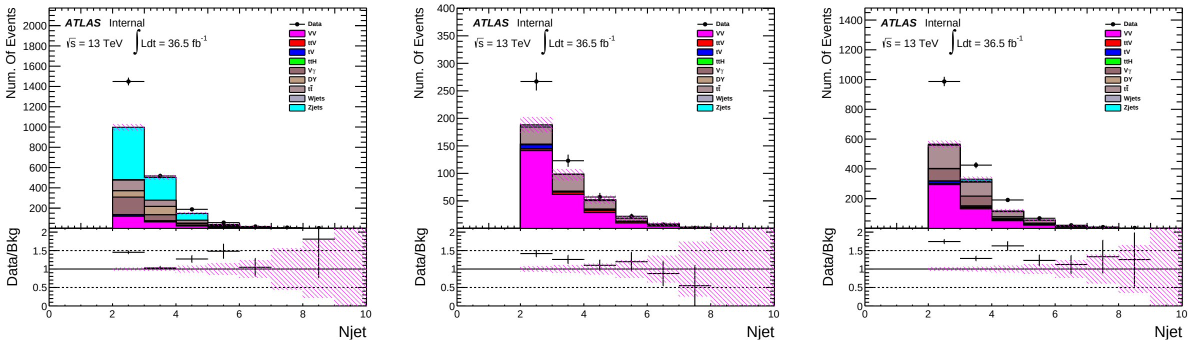

Figure 4: Distributions of number of jets at pre-selection level with data and pure background MC samples. Left: ee, middle: $\mu\mu$, right:$e\mu$.

5.1 QmisID estimation

The event selection requires two same sign leptons which rejects most of the background contributions. Still, there are some reducible backgrounds coming from the fact that one of the leptons can have the QmisID. According to previous 8 TeV ATLAS studies, muon QmisID is immeasurably small [13], therefore we only consider electron QmisID in this analysis.

There are two main contributions for electron QmisID. The main contribution comes from the radiation of a hard photon (hard Bremsstrahlung process) when the electron passes through materials. This photon then converts into e^+e^- pair and when the EM cluster is associated with the wrong electron's track, an electron of the opposite charge with respect to the original electron maybe reconstructed, leading to QmisID. The hard Bremsstrahlung process depends on the amount of interaction materials in the detector, which in turn depends on $|\eta|$, thus the QmisID rates are expected to have a strong $|\eta|$ dependence. The second and minor contribution comes from the measurement error for a lightly curved track or when the track-cluster association is wrong. This effect is important at high transverse momentum, thus the QmisID rates are also expected to have a small dependence on p_T.

Electrons coming from the leptonic decay of the Z boson are used to measure the QmisID rates in data using a Likelihood technique [14]. The QmisID rates are measured selecting events with two good electrons originating from a Z decay. Events are selected with the standard analysis selections requiring two nominal leptons with an invariant mass within ±20GeV of the Z mass window . These events are then divided into same sign events (SS) and opposite sign events (OS) depending on the charges of two nominal leptons. These events are dominated by Z boson decay events and the small remaining backgrounds are subtracted using side-band method. The two dimensional likelihood method defines the bin boundaries as [0., 0.80, 1.14, 1.60, 1.80, 2.00, 2.20, 2.30, 2.40, 2.50] on electron η and [10, 60, 90, 130, 1000] GeV on electron p_T.

After measuring the QmisID rates, a closure test has been done by comparing the rates measured with likelihood method and truth-matching method based on simulated electron samples from Z boson decays. **since we follow the same tight definitions of electrons as ttH group, we just borrow their results**

5.2 Jet fakes estimation with fake factor method

Mis-identification is an important source of background for physics analysis using particle-level identification criteria. In the case of the di-lepton analysis presented in this analysis, this background arises from $t\bar{t}$(semi-leptonic) and W+jet events in which a jet is misidentified as a lepton. The motivation to use fake factor method is the rate of mis-identification may not be accurately modeled in the MC.

5.2.1 Estimation strategy

This measurement is based on the assumption that the fake factor is stable with respect to the jet multiplicity which was tested in ttH analysis in run-1. The fake factor is defined as the ratio of number of SS events with two tight leptons over events with one tight lepton and one anti-tight lepton:

$$\theta_\ell = \frac{N_{\ell\ell}}{N_{\ell\not\ell}} \tag{1}$$

where ℓ is tight e or μ, $\not\ell$ anti-tight lepton which is not used for trigger matching. The definitions of ℓ and $\not\ell$ follow:

	tight electron	anti-tight electron
ID	TightLH	fail TightLH
isolation	isolationFixedCutTight	NO
Vertex	$\lvert z_0 sin\theta\rvert < 0.5$, $\lvert d_0/\sigma(d_0)\rvert < 5$	NO

Table 6: definitions of tight electrons and anti-tight electrons

	tight muon	anti-tight muon
ID	Tight	NO
isolation	isolationFixedCutTightTrackOnly	fail isolationFixedCutTightTrackOnly
Vertex	$\lvert z_0 sin\theta\rvert < 0.5$, $\lvert d_0/\sigma(d_0)\rvert < 3$	NO

Table 7: definitions of tight muons and anti-tight muons

Both tight and anti-tight leptons have to pass object definitions. Below demonstrates how to estimate jet fakes using fake factor method, please note that: since there are two categories in signal region, fake factor method is repeated two times. For mH=260 and 300 GeV, fake factor is estimated in N_{jet} == 1 region, and apply fake factor to $N_{\text{jet}} \geq 2$ region; while for mH=400, 500 GeV and non-res, fake factor is estimated in $1 \leq N_{\text{jet}} \leq 2$ region, and apply it in $N_{\text{jet}} \geq 3$ region. Below only demonstrates fake factor method which is corresponding to the high mass search. Fake factor is estimated from low jet multiplicity region and can be written as:

$$\theta_e(\leq 2\text{jets}) = \frac{N_{ee}^{\text{data}} - N_{ee}^{\text{prompt SS}} - N_{ee}^{\text{QmisID}}}{N_{e\not e}^{\text{data}} - N_{e\not e}^{\text{prompt SS}} - N_{e\not e}^{\text{QmisID MC}}}(\leq 2\text{jets}) \tag{2}$$

$$\theta_\mu(\leq 2\text{jets}) = \frac{N_{\mu\mu}^{\text{data}} - N_{\mu\mu}^{\text{prompt SS}}}{N_{\mu\not\mu}^{\text{data}} - N_{\mu\not\mu}^{\text{prompt SS}}}(\leq 2\text{jets}) \tag{3}$$

There are two kinds of subtractions. Prompt SS consists of ttV, VV, tV and ttH. Truth matching is always applied in prompt SS background. And the prompt opposite-sign events with QmisID(for electrons only) are estimated with data and noted N_{ee}^{QmisID}. In $\ell\not{\ell}$ events, $N_{e\not{e}}^{\text{QmisID MC}}$ is estimated using MC, in which two electrons(in $e^{\pm}e^{\pm}$) or the electrons(in $e^{\pm}\mu^{\pm}$) match real prompt leptons($\Delta R < 0.2$). Because of these subtractions, there is no overlap between QmisID and jet fakes estimation. Following tables present various numbers of events in different fake factor control regions.

Selections		VV	$t\bar{t}V$	tV	$t\bar{t}H$	$V\gamma$	QmisID	Data
N_{jet} ==1	ee	212.86±18.32	1.06±0.06	19.31±2.38	0.10±0.05	229.49±13.27	1947.63±7.65	3187.00±56.45
	$e\not{e}$	58.63±3.90	0.22±0.03	17.26±2.08	0.00±0.00	180.27±13.91	2863.15±440.51	4513.00±67.18

Table 8: Observed number of data and expected events yields in low jet multiplicity region, which is used for fake factor calculation of electron in low mass search. Uncertainties are statistical.

Selections		VV	$t\bar{t}V$	tV	$t\bar{t}H$	$V\gamma$	Data
N_{jet} ==1	$\mu\mu$	240.93±8.40	1.33±0.08	2.58±0.64	0.09±0.04	0.00±0.00	459.00±21.42
	$\mu\not{\mu}$	66.51±5.54	0.09±0.02	19.62±2.27	0.00±0.00	1.60±0.70	629.00±25.08

Table 9: Observed number of data and expected events yields in low jet multiplicity region, which is used for fake factor calculation of muon in low mass search. Uncertainties are statistical.

Selections		VV	$t\bar{t}V$	tV	$t\bar{t}H$	$V\gamma$	QmisID	Data
$1 \leq N_{\text{jet}} \leq 2$	ee	322.68±19.00	3.58±0.14	30.06±2.85	0.36±0.10	349.88±16.93	2703.98±9.17	4565.00±67
	$e\not{e}$	87.44±5.56	0.68±0.05	29.35±2.81	0.05±0.03	253.00±16.01	3866.53±472.71	6119.00±78

Table 10: Observed number of data and expected events yields in low jet multiplicity region, which is used for fake factor calculation of electron in high mass search. Uncertainties are statistical.

Selections		VV	$t\bar{t}V$	tV	$t\bar{t}H$	$V\gamma$	Data
$1 \leq N_{\text{jet}} \leq 2$	$\mu\mu$	385.76±10.30	4.47±0.15	8.59±1.41	0.42±0.11	0.57±0.56	720.00±26.83
	$\mu\not{\mu}$	91.68±6.08	0.35±0.03	45.99±3.44	0.06±0.03	10.05±5.70	1090.00±33.02

Table 11: Observed number of data and expected events yields in low jet multiplicity region, which is used for fake factor calculation of muon in high mass search. Uncertainties are statistical.

In summary, the fake factors of electron and muon with different N_{jet} requirements are found in Tab. 12. Then to predict number of jet fakes in high jet multiplicity region, following calculations will be used:

$$N_{ee}^{\text{fakes}}(\geq 3\text{jets}) = (N_{e\not{e}}^{\text{data}} - N_{e\not{e}}^{\text{prompt SS}} - N_{e\not{e}}^{\text{QmisID MC}})(\geq 3\text{jets}) \times \theta_e \tag{4}$$

$$N_{\mu\mu}^{\text{fakes}}(\geq 3\text{jets}) = (N_{\mu\not{\mu}}^{\text{data}} - N_{\mu\not{\mu}}^{\text{prompt SS}})(\geq 3\text{jets}) \times \theta_\mu \tag{5}$$

$$N_{e\mu}^{\text{fakes}}(\geq 3\text{jets}) = (N_{e\not{\mu}} - N_{e\not{\mu}}^{\text{prompt SS}} - N_{e\not{\mu}}^{\text{QmisID}})(\geq 3\text{jets}) \times \theta_\mu + (N_{\not{e}\mu} - N_{\not{e}\mu}^{\text{prompt SS}} - N_{\not{e}\mu}^{\text{QmisID MC}})(\geq 3\text{jets}) \times \theta_e \tag{6}$$

Selections	Fake factor	Value
N_{jet} ==1	θ_e	0.56±0.04
	θ_μ	0.40±0.08
$1 \leq N_{\text{jet}} \leq 2$	θ_e	0.61±0.04
	θ_μ	0.34±0.06

Table 12: Summary of fake factors of electron and muon with different N_{jet} requirements. Uncertainties are statistical.

Tab. 13 and Tab. 14 present number of events with different N_{jet} requirements in control regions.

Selections		VV	$t\bar{t}V$	tV	$t\bar{t}H$	$V\gamma$	QmisID	Data
$N_{\text{jet}} \geq 2$	$e\not{e}$	52.13±4.87	2.14±0.11	19.53±2.27	0.39±0.12	108.37±9.22	1498.91±193.01	2542.00±50.42
	$\mu\not{\mu}$	46.35±3.40	1.75±0.10	46.25±3.38	0.71±0.12	8.50±5.66	-	1047.00±32.36
	$\not{e}\mu$	51.91±3.52	2.27±0.11	23.57±2.38	0.47±0.11	78.97±10.48	355.59±47.41	1097.00±33.12
	$e\not{\mu}$	24.11±2.62	0.86±0.06	32.90±3.67	0.33±0.20	2.41±0.98	0.00±0.00	590.00±24.29

Table 13: Observed number of data and expected events yields in high jet multiplicity region, which is used to predict fakes in low mass search. Uncertainties are statistical.

Selections		VV	$t\bar{t}V$	tV	$t\bar{t}H$	$V\gamma$	QmisID	Data
$N_{\text{jet}} \geq 3$	$e\not{e}$	23.32±2.83	1.68±0.10	7.44±1.25	0.34±0.11	35.64±4.71	495.52±88.56	936.00±30.59
	$\mu\not{\mu}$	21.18±2.28	1.49±0.09	19.88±2.18	0.66±0.12	0.06±0.04	-	586.00±24.21
	$\not{e}\mu$	21.71±2.01	1.78±0.10	9.77±1.54	0.46±0.11	23.89±4.95	205.90±44.48	460.00±21.45
	$e\not{\mu}$	8.97±1.24	0.75±0.06	19.69±3.18	0.29±0.20	1.17±0.41	0.00±0.00	321.00±17.92

Table 14: Observed number of data and expected events yields in high jet multiplicity region, which is used to predict fakes in high mass search. Uncertainties are statistical.

After all the subtractions, and multiply with corresponding fake factors, the number of jet fakes in three channels are summarized in Tab. 15.

Selections	$N_{\text{jet}} \geq 2$			$N_{\text{jet}} \geq 3$		
	ee	$\mu\mu$	$e\mu$	ee	$\mu\mu$	$e\mu$
Event yield	481.89±111.87	377.37±13.28	538.92±34.45	226.95±57.26	184.53±8.30	218.51±30.94

Table 15: Estimated jet fakes in three channels with different selections. Uncertainties are statistical.

5.2.2 Systematics

There are several sources of systematic uncertainties on estimated fake factors:

- **Statistics**: Statistical uncertainty in low multiplicity region will propagate to θ_e and θ_μ.

- **QmisID**: The contribution of charge-mis-identification is significant in ee channel, the full uncertainty on this background is propagated to θ_e. Therefore, the uncertainty on QmisID background in ee and $e\mu$ are counted on estimated jet fakes.
- **θ_ℓ syst.(closure test)**: There should be some uncertainty on extrapolation from low jet multiplicity region to high jet multipicity region. This is estimated by simulated W+jets, and the difference between predicted number of fakes and that of real fakes are considered as systematics, which will be translated on θ_e and θ_μ.
- **Sample dependence**: The fake factor is estimated in low jet multiplicity region with b veto, which is expected to be W+jets dominant. However, $t\bar{t}$ process can contribute and be underestimated. In order to estimate such uncertainty, fake factor method is repeated without b veto, and the relative variation is considered as uncertainty on θ_ℓ.

All the systematics on θ_e and θ_μ are summarized in Tab. 16 and Tab. 17,respectively.

	N_{jet} ==1	$1 \leq N_{\text{jet}} \leq 2$
Statistics	7.1	6.6
QmisID	25.0	23.0
θ_ℓ syst.	27.1	25.4
Sample dependence	39.3	26.2
Total	54.4	43.6

Table 16: Summary of systematic uncertainty on θ_e with different N_{jet} selections(in %).

	N_{jet} ==1	$1 \leq N_{\text{jet}} \leq 2$
Statistics	20.0	17.6
θ_ℓ syst.	2.1	30.4
Sample dependence	57.5	52.9
Total	60.9	63.5

Table 17: Summary of systematic uncertainty on θ_μ with different N_{jet} selections(in %).

5.2.3 Event yields at pre-selection level with data-driven methods

After performing all the methods disscussed above, we present the event yields at pre-selection level. Concerning about the uncertainty on estimated jet fakes, there is one additional uncertainty that is due to size of high multiplicity control region. It is approximated by $\theta_\ell \times \sqrt{N_{\ell\not\ell}^{\geq 2\text{jet}(3\text{jet})}}$. So assuming it is independent with systematical uncertainty on θ_ℓ, the final error on estimated jet fakes is: $\sqrt{(\theta_\ell^{\text{sys.}} \times N_{\text{jet fakes}}^{\text{nominal}})^2 + \theta_\ell \times N_{\text{jet fakes}}^{\text{nominal}}}$, where $\theta_\ell^{\text{sys.}}$ is the systematical uncertainty on θ_ℓ, and $N_{\text{jet fakes}}^{\text{nominal}}$ number of jet fakes using median θ_ℓ. Tab. 18 and Tab. 19 show event yields by the requirement of $N_{\text{jet}} \geq 2$ and $N_{\text{jet}} \geq 3$, respectively. Good agreements are observed between data and total estimated backgrounds within uncertainties. Each region is divided into three channel considering the different flavor pairs of leptons, i.e. ee, $\mu\mu$ and $e\mu$. It has been checked that signal fraction is below 1%. The comparisons between data and estimated backgrounds are shown in Fig. 6. More variables are shown in Fig. 11. Good agreements are observed between data and total estimated backgrounds within uncertainties. More plots are presented in Fig. 12.

	ee	$\mu\mu$	$e\mu$
Jet fakes	481.89±262.66	377.37±230.15	538.93±220.40
PromptSS	236.58±7.15	286.67±7.88	566.63±10.79
$V + \gamma$	183.61±12.15	0.58±0.56	175.56±17.62
QmisID	1144.24±6.34	0.00±0.00	197.81±2.22
Total predicted	2046.32±263.12	664.63±230.28	1478.92±221.38
Observed	2167.00±46.55	488.00±22.09	1660.00±40.74

Table 18: Event yields at pre-selection level, corresponding to $N_{\text{jet}} \geq 2$. Uncertainties include all systematics.

	ee	$\mu\mu$	$e\mu$
Jet fakes	226.94±99.64	184.53±117.44	218.51±82.23
PromptSS	113.22±4.79	132.36±5.00	266.83±7.38
$V + \gamma$	63.21±6.11	0.01±0.01	81.00±14.70
QmisID	387.69±3.81	0.00±0.00	88.89±1.51
Total predicted	791.07±100.02	316.89±117.55	655.23±83.87
Observed	789.00±28.09	227.00±15.07	717.00±26.78

Table 19: Event yields at pre-selection level, corresponding to $N_{\text{jet}} \geq 3$. Uncertainties include all systematics.

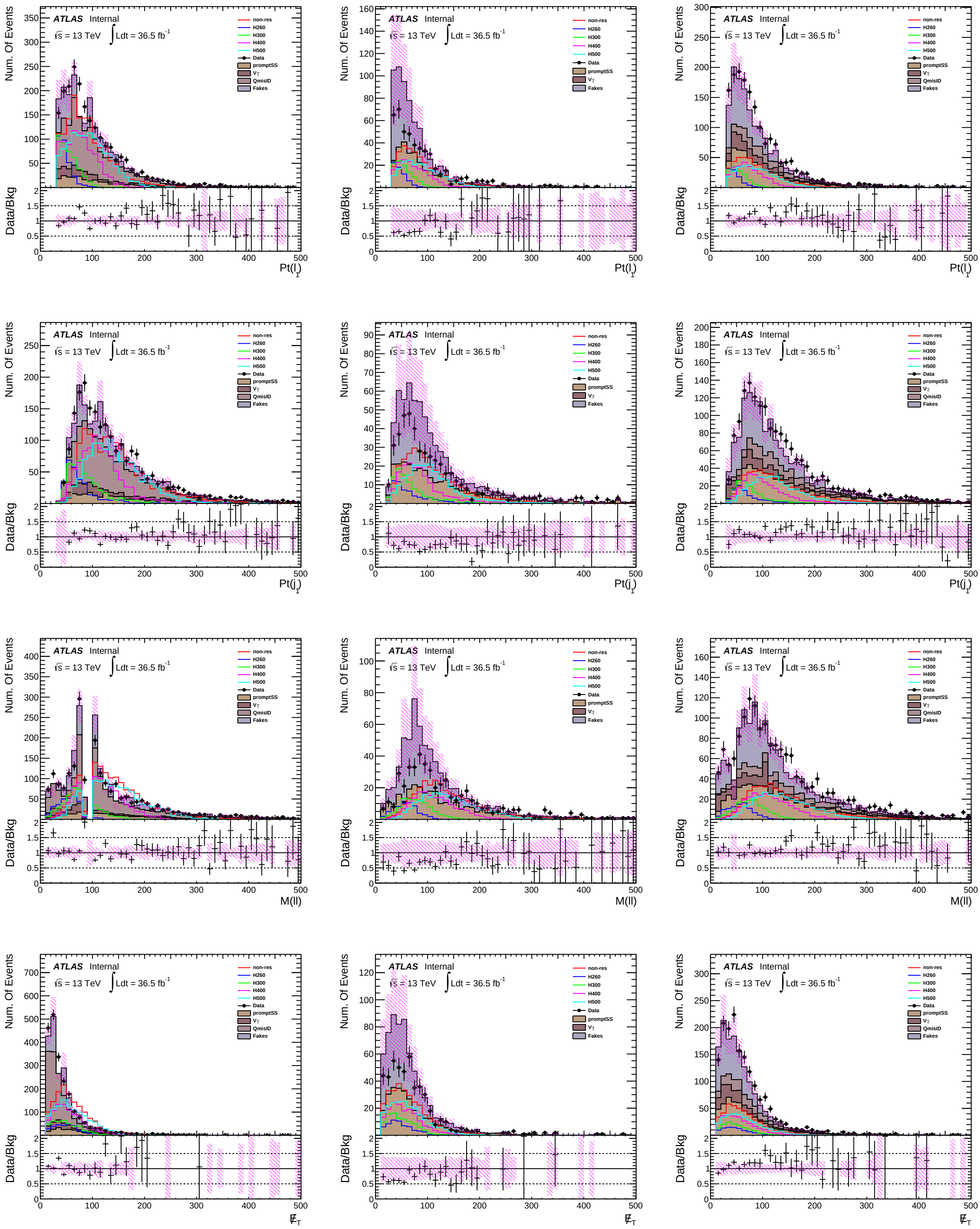

Figure 5: The comparisons between data and backgrounds at pre-selection level, corresponding to $N_{\text{jet}} \geq 2$. Left: ee, middle: $\mu\mu$, right: $e\mu$. From top to bottom, Pt of leading lepton, Pt of leading jet, invariant mass of two leptons and missing energy are shown. The backgrounds consist of promptSS(which contribute two prompt same-signed leptons), QmisID and fakes(jet faking lepton). Uncertainties include all systematics.

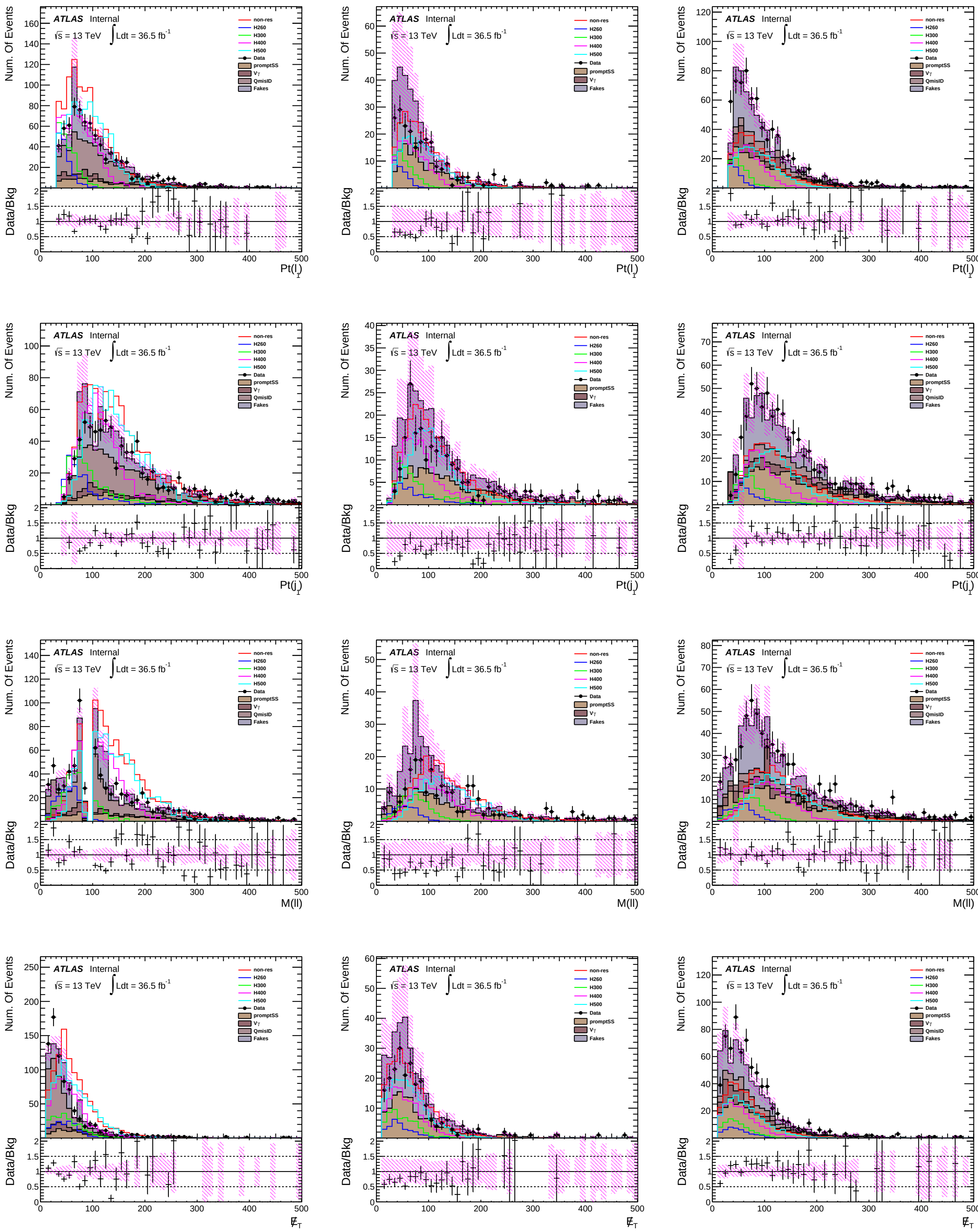

Figure 6: The comparisons between data and backgrounds at pre-selection level, corresponding to $N_{\text{jet}} \geq 3$. Left: ee, middle: $\mu\mu$, right: $e\mu$. From top to bottom, Pt of leading lepton, Pt of leading jet, invariant mass of two leptons and missing energy are shown. The backgrounds consist of promptSS(which contribute two prompt same-sign leptons), QmisID and fakes(jet faking lepton). Uncertainties include all systematics.

6 Signal optimization

In order to enhance signal sensitivity, optimizations are performed at pre-selection level. Firstly, a MVA method was used to determine the separating power of different kinematic variables. And correlations between all the variables are taken into account. Eventually, top five kinematic variables are used to form optimization selections. The five optmization variables are $M(\ell\ell)$, $\Delta R_{min}(\ell_2, j)$, $\Delta R_{min}(\ell_1, j)$, $M_{\ell_1 jj}$ and $M(all)$, which have strong separating power and low correlations between them(Fig. 6). In general, $M(\ell\ell)$ and $M_{\ell_1 jj}$ are sensitive to low mass points, while the remaining are sensitive to high mass and non-res signal.
The TMVA package(CutsSA option) is used to achieve optimal cuts. All the backgrounds: promptSS, $V\gamma$, QmisID and fakes are included in the training. In order to reduce the dependence on the order of cuts, the framework is used to train only 2 cuts each time. Then assigning a common signal efficiency working point, signal and all background samples are evaluated(pass or not) event by event. For each signal efficiency WP., significance($S/\sqrt{B}$) is calculated. Finally, the signal efficiency WP. that has highest significance is selected. Based on this common WP., optimal cut values can be achieved. Fig. 6 shows the significance scan as a function of signal efficiency WP. for $\mu\mu$ in the non-resonant signal optimisation. It is repeated for remaining channels and other mass points.
Eventually considering continuity of cut values from low to high(and non-res)mass points, some tuning are performed. The selections are summarized in Tab. 20 and Tab. 21, corresponding to low and high mass search, respectively. In general, it is the most sensitive in $\mu\mu$ channel, as there is negligible QmisID background, as well as much less fakes.

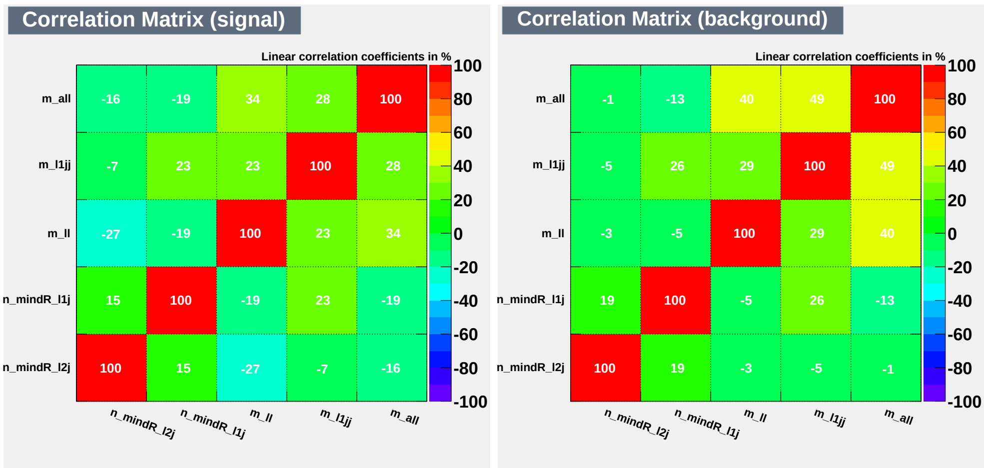

Figure 7: Correlation check of input training variables.

7 Statistical interpretation

A likelihood ratio based test statistic is used, which is defined as follows:

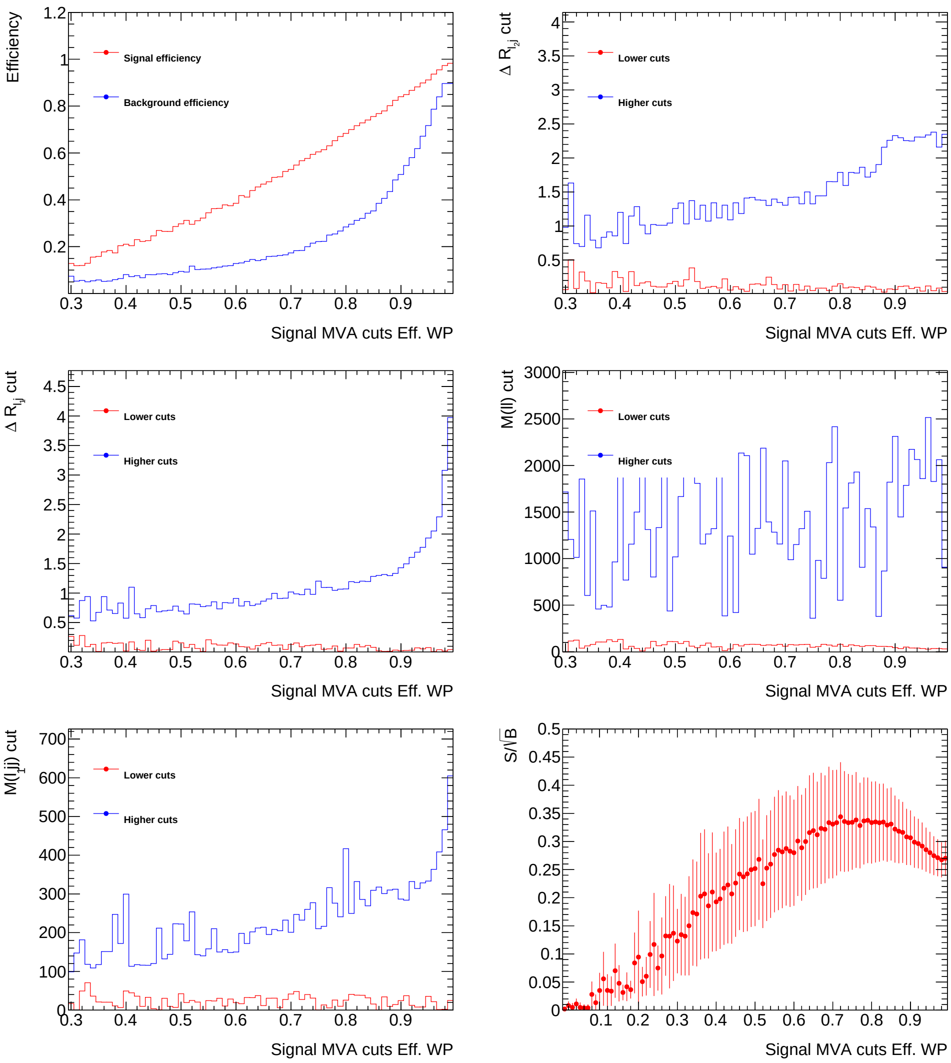

Figure 8: The significance scan as a function of efficiency for $\mu\mu$ in non-resonant signal search. Statistical uncertainties on the background and the signal are considered. The 0.72 working point is chosen for $\mu\mu$ channel in the non-resonant signal optimisation.

$$\tilde{q}_\mu = \begin{cases} -2\ln\frac{\mathcal{L}(\mu,\hat{\hat{\theta}}(\mu))}{\mathcal{L}(0,\hat{\hat{\theta}}(0))} & \text{if } \hat{\mu} < 0 \\ -2\ln\frac{\mathcal{L}(\mu,\hat{\hat{\theta}}(\mu))}{\mathcal{L}(\hat{\mu},\hat{\hat{\theta}})} & \text{if } 0 \leq \hat{\mu} \leq \mu \\ 0 & \text{if } \hat{\mu} > \mu \end{cases}$$

where single hat stands for unconditional fit and double hat for conditional fit (i.e., μ is fixed to a certain value). With this test statistic, one can derive the upper limits of the cross section production times the branching ratio for each scanned mass point by using the CL_s method [15] under the asymptotic approximation [16].

	Channel	$\Delta R_{min}(\ell_1, j)$	$M(ll)$	$M_{\ell_1 jj}$	$M(all)$
mH300	ee				
	$\mu\mu$				
	$e\mu$				
mH260	ee				
	$\mu\mu$				
	$e\mu$				

Table 20: Summary of optimization selections for each channel of low mass points.

	Channel	$\Delta R_{min}(\ell_2, j)$	$\Delta R_{min}(\ell_1, j)$	$M(ll)$	$M_{\ell_1 jj}$
Non-res	ee	(0.29, 1.87)	(0.27, 1.17)	(70, 500)	(30, 300)
	$\mu\mu$	(0.14, 1.42)	(0.09, 0.97)	(72.5, 500)	(27.4, 250)
	$e\mu$	(0.08, 1.35)	(0.08, 1.39)	(55, 492.8)	(27.9, 222.6)
mH500	ee				
	$\mu\mu$				
	$e\mu$				
mH400	ee				
	$\mu\mu$				
	$e\mu$				

Table 21: Summary of optimization selections for each channel of high mass points and non-res.

	promptSS	$V\gamma$	QmisID	Fakes	Total bkg	signal	Total predicted	Observed
$\Delta R_{min}(l_2, j)$	81.05±3.86	38.34±4.58	249.28±2.99	207.25±91.06	575.92±91.30	1.96±0.07	577.87±91.30	0±0.00
$\Delta R_{min}(l_1, j)$	27.67±2.27	13.21±2.65	73.73±1.56	47.81±21.53	162.41±21.87	1.52±0.06	163.93±21.87	0±0.00
$M(\ell\ell)$	21.21±2.10	7.54±2.20	49.76±1.29	20.00±9.39	98.51±9.96	1.32±0.06	99.83±9.96	0±0.00
$M(l_1 jj)$	14.37±1.33	6.25±2.16	39.72±1.11	17.71±8.39	78.05±8.84	1.22±0.06	79.27±8.84	0±0.00

Table 22: (un)Blinded results of non-res search in ee channel.

7.1 Search for non-resonant Higgs boson pair production

Assuming $\sigma(pp \to hh)$ being $1pb$, the 95% CL_s upper limit on the non-resonant Higgs pair production process $pp \to hh \to WW^*WW^*$ is XXX fb.

7.2 Search for resonant Higgs boson pair production

The 95% CL$_s$ upper limit on the cross section times branching ratio of $H \to hh$ as a function of m_H is shown in Figure 9.

Also, using the 95% CLs upper limits, one can make exclusions in 2HDM phase space if considering the heavy resonance that we look for as the CP-even heavy Higgs, as shown in Fig. 10 for type I, II, III and IV.

	promptSS	$V+\gamma$	QmisID	Fakes	Total bkg	signal	Total predicted	Observed
$\Delta R_{min}(l_2, j)$	66.43±3.24	0.01±0.01	0.00±0.00	104.73±66.77	171.17±66.85	4.17±0.10	175.34±66.85	0±0.00
$\Delta R_{min}(l_1, j)$	22.42±1.84	0.00±0.00	0.00±0.00	35.56±22.84	57.97±22.92	3.36±0.09	61.33±22.92	0±0.00
$M(\ell\ell)$	16.97±1.66	0.00±0.00	0.00±0.00	26.64±17.18	43.62±17.26	3.06±0.09	46.68±17.26	0±0.00
$M(l_1 jj)$	11.48±1.19	0.00±0.00	0.00±0.00	20.83±13.49	32.30±13.54	2.66±0.08	34.96±13.54	0±0.00

Table 23: (un)Blinded results of non-res search in $\mu\mu$ channel.

	promptSS	$V+\gamma$	QmisID	Fakes	Total bkg	signal	Total predicted	Observed
$\Delta R_{min}(l_2, j)$	125.37±4.75	31.79±5.52	45.29±1.09	126.46±46.57	328.91±47.15	5.68±0.14	334.59±47.15	0±0.00
$\Delta R_{min}(l_1, j)$	69.72±3.62	18.13±4.31	23.50±0.77	61.77±22.92	173.12±23.62	4.97±0.13	178.10±23.62	0±0.00
$M(\ell\ell)$	58.81±3.35	13.74±3.92	20.54±0.73	45.13±17.01	138.21±17.79	4.77±0.13	142.98±17.79	0±0.00
$M(l_1 jj)$	38.51±2.74	8.11±2.77	13.45±0.54	38.29±14.51	98.36±15.04	4.19±0.12	102.55±15.04	0±0.00

Table 24: (un)Blinded results of non-res search in $e\mu$ channel.

Figure 9: for ee channel only, for $\mu\mu$ channel only, for $e\mu$ channel only, for combined. **??** for ee channel only, **??** for $\mu\mu$ channel only, **??** for $e\mu$ channel only, **??** for combined.

Figure 10: 2HDM interpretation plots: **??** for type I, **??** for type II, **??** for type III, **??** for type IV.

The upper limits for non-res as well as resonance are shown in Table 25.

	Higgs pair	260 GeV	300 GeV	400 GeV	500 GeV
Median					
Observed					
$+2\sigma$					
$+1\sigma$					
-1σ					
-2σ					

Table 25: Combined exclusion limits at the 95% CL for the production cross section of a gluon fusion produced H boson times its branching ratio to hh.

8 Conclusions

Acknowledgements

The `atlaslatex` package contains the acknowledgements that were valid at the time of the release you are using. These can be found in the `acknowledgements` subdirectory. When your ATLAS paper or PUB/CONF note is ready to be published, download the latest set of acknowledgements from:
https://twiki.cern.ch/twiki/bin/view/AtlasProtected/PubComAcknowledgements

The supporting notes for the analysis should also contain a list of contributors. This information should usually be included in `mydocument-metadata.tex`. The list should be printed either here or before the table of contents.

Appendix

A MadGraph5 card used for resonance signal

The run card used for generating heavy resonant scalar at the mass point of 300 GeV is attached.

```
#***********************************************************************
#                        MadGraph5_aMC@NLO                             *
#                                                                      *
#                      run_card.dat aMC@NLO                            *
#                                                                      *
#  This file is used to set the parameters of the run.                 *
#                                                                      *
#  Some notation/conventions:                                          *
#                                                                      *
#   Lines starting with a hash (#) are info or comments                *
#                                                                      *
#   mind the format:   value    = variable     ! comment               *
#***********************************************************************
#
#*******************
# Running parameters
#*******************
#
#***********************************************************************
# Tag name for the run (one word)                                      *
#***********************************************************************
  tag_1     = run_tag ! name of the run
#***********************************************************************
# Number of LHE events (and their normalization) and the required      *
# (relative) accuracy on the Xsec.                                     *
# These values are ignored for fixed order runs                        *
#***********************************************************************
  10000       = nevents ! Number of unweighted events requested
    -1 = req_acc ! Required accuracy (-1=auto determined from nevents)
    -1 = nevt_job! Max number of events per job in event generation.
                 !  (-1= no split).
#***********************************************************************
# Normalize the weights of LHE events such that they sum or average to *
# the total cross section                                              *
#***********************************************************************
 average = event_norm      ! average or sum
#***********************************************************************
```

```
# Number of points per itegration channel (ignored for aMC@NLO runs)   *
#***********************************************************************
 0.01   = req_acc_FO       ! Required accuracy (-1=ignored, and use the
                     ! number of points and iter. below)
# These numbers are ignored except if req_acc_FO is equal to -1
 5000   = npoints_FO_grid  ! number of points to setup grids
 4      = niters_FO_grid   ! number of iter. to setup grids
 10000  = npoints_FO       ! number of points to compute Xsec
 6      = niters_FO        ! number of iter. to compute Xsec
#***********************************************************************
# Random number seed                                                   *
#***********************************************************************
   2016      = iseed   ! rnd seed (0=assigned automatically=default))
#***********************************************************************
# Collider type and energy                                             *
#***********************************************************************
    1   = lpp1    ! beam 1 type (0 = no PDF)
    1   = lpp2    ! beam 2 type (0 = no PDF)
   6500      = ebeam1  ! beam 1 energy in GeV
   6500      = ebeam2  ! beam 2 energy in GeV
#***********************************************************************
# PDF choice: this automatically fixes also alpha_s(MZ) and its evol.  *
#***********************************************************************
 lhapdf    = pdlabel   ! PDF set
 11000     = lhaid     ! if pdlabel=lhapdf, this is the lhapdf number
#***********************************************************************
# Include the NLO Monte Carlo subtr. terms for the following parton    *
# shower (HERWIG6 | HERWIGPP | PYTHIA6Q | PYTHIA6PT | PYTHIA8)         *
# WARNING: PYTHIA6PT works only for processes without FSR!!!!          *
#***********************************************************************
 HERWIGPP    = parton_shower
#***********************************************************************
# Renormalization and factorization scales                             *
# (Default functional form for the non-fixed scales is the sum of      *
# the transverse masses of all final state particles and partons. This *
# can be changed in SubProcesses/set_scales.f)                         *
#***********************************************************************
 .true.    = fixed_ren_scale  ! if .true. use fixed ren scale
 .true.    = fixed_fac_scale  ! if .true. use fixed fac scale
 130.0     = muR_ref_fixed    ! fixed ren reference scale
 130.0     = muF1_ref_fixed   ! fixed fact reference scale for pdf1
 130.0     = muF2_ref_fixed   ! fixed fact reference scale for pdf2
#***********************************************************************
# Renormalization and factorization scales (advanced and NLO options)  *
#***********************************************************************
 .true.    = fixed_QES_scale  ! if .true. use fixed Ellis-Sexton scale
 130.0     = QES_ref_fixed    ! fixed Ellis-Sexton reference scale
```

```
 1        = muR_over_ref     ! ratio of current muR over reference muR
 1        = muF1_over_ref    ! ratio of current muF1 over reference muF1
 1        = muF2_over_ref    ! ratio of current muF2 over reference muF2
 1        = QES_over_ref     ! ratio of current QES over reference QES
#***********************************************************************
# Reweight flags to get scale dependence and PDF uncertainty          *
# For scale dependence: factor rw_scale_up/down around central scale  *
# For PDF uncertainty: use LHAPDF with supported set                  *
#***********************************************************************
 .true.   = reweight_scale   ! reweight to get scale dependence
  0.5     = rw_Rscale_down   ! lower bound for ren scale variations
  2.0     = rw_Rscale_up     ! upper bound for ren scale variations
  0.5     = rw_Fscale_down   ! lower bound for fact scale variations
  2.0     = rw_Fscale_up     ! upper bound for fact scale variations
 .false.  = reweight_PDF     ! reweight to get PDF uncertainty
 11001    = PDF_set_min      ! First of the error PDF sets
 11052    = PDF_set_max      ! Last of the error PDF sets
#***********************************************************************
# Merging - WARNING! Applies merging only at the hard-event level.    *
# After showering an MLM-type merging should be applied as well.      *
# See http://amcatnlo.cern.ch/FxFx_merging.htm for more details.      *
#***********************************************************************
 0        = ickkw            ! 0 no merging, 3 FxFx merging, 4 UNLOPS
#***********************************************************************
#
#***********************************************************************
# BW cutoff (M+/-bwcutoff*Gamma)                                      *
#***********************************************************************
 15  = bwcutoff
#***********************************************************************
# Cuts on the jets                                                    *
# Jet clustering is performed by FastJet.
# When matching to a parton shower, these generation cuts should be   *
# considerably softer than the analysis cuts.                         *
# (more specific cuts can be specified in SubProcesses/cuts.f)        *
#***********************************************************************
  -1  = jetalgo   ! FastJet jet algorithm (1=kT, 0=C/A, -1=anti-kT)
 0.4  = jetradius ! The radius parameter for the jet algorithm
  10  = ptj       ! Min jet transverse momentum
  -1  = etaj      ! Max jet abs(pseudo-rap) (a value .lt.0 means no cut)
#***********************************************************************
# Cuts on the charged leptons (e+, e-, mu+, mu-, tau+ and tau-)       *
# (more specific gen cuts can be specified in SubProcesses/cuts.f)    *
#***********************************************************************
   0  = ptl     ! Min lepton transverse momentum
  -1  = etal    ! Max lepton abs(pseudo-rap) (a value .lt.0 means no cut)
   0  = drll    ! Min distance between opposite sign lepton pairs
```

```
  0  = drll_sf ! Min distance between opp. sign same-flavor lepton pairs
  0  = mll     ! Min inv. mass of all opposite sign lepton pairs
 30  = mll_sf  ! Min inv. mass of all opp. sign same-flavor lepton pairs
#*********************************************************************
# Photon-isolation cuts, according to hep-ph/9801442                 *
# When ptgmin=0, all the other parameters are ignored                *
#*********************************************************************
 20  = ptgmin    ! Min photon transverse momentum
 -1  = etagamma  ! Max photon abs(pseudo-rap)
0.4  = R0gamma   ! Radius of isolation code
1.0  = xn        ! n parameter of eq.(3.4) in hep-ph/9801442
1.0  = epsgamma  ! epsilon_gamma parameter of eq.(3.4) in hep-ph/9801442
.true.  = isoEM  ! isolate photons from EM energy (photons and leptons)
#*********************************************************************
# Maximal PDG code for quark to be considered a jet when applying cuts.*
# At least all massless quarks of the model should be included here.   *
#*********************************************************************
 4 = maxjetflavor
#*********************************************************************
# For aMCfast+APPLGRID use in PDF fitting (http://amcfast.hepforge.org)*
#*********************************************************************
 0 = iappl   ! aMCfast switch (0=OFF, 1=prepare APPLgrids, 2=fill grids)
#*********************************************************************
```

B Cutflow for signal

The cut-flow for signal samples are attached in Tab 26, numbers in brackets are corresponding to weighted events at the luminosity of 1 fb^{-1}.

	Non-resonant	260 GeV	300 GeV	400 GeV	500 GeV
AOD	991000	194000	199000	189000	100000
HIGG8D1	513929(0.702136)	97527(2.0683)	103755(2.21802)	104916(2.30827)	57164(1.21095)
Trigger	428667(0.572711)	55088(1.255286)	63055(1.444759)	71526(1.675622)	41064(0.918026)
(loose)NLeptons==2	150872(0.270185)	28633(0.644259)	31844(0.715429)	34128(0.793765)	18188(0.405493)
(tight)NLeptons==2	116252(0.207964)	23415(0.46967)	26230(0.534528)	28775(0.60603)	15468(0.310993)
Same sign	115430(0.207157)	23322(0.467951)	26134(0.532597)	28639(0.604213)	15383(0.309272)
Trigger Match	113554(0.200589)	22484(0.44811)	25386(0.511928)	28295(0.596558)	15235(0.305797)
$>= 3 jets$	85641(0.132106)	7571(0.145321)	11268(0.224815)	17675(0.358082)	11001(0.219792)
B veto	78086(0.122304)	7084(0.135551)	10528(0.210555)	16448(0.333617)	10138(0.200973)
$MET > 10\,GeV$	76623(0.118167)	6794(0.129542)	10126(0.20165)	15979(0.323654)	9910(0.196406)

Table 26: event yield of non-resonant and resonant signal samples

C Plots in Control Regions

High N_{jet} CR

The comparisons between MC+data-driven backgrounds and data set for various kinematics are made in High N_{jet} CR. Good agreements can be seen in Fig 11.

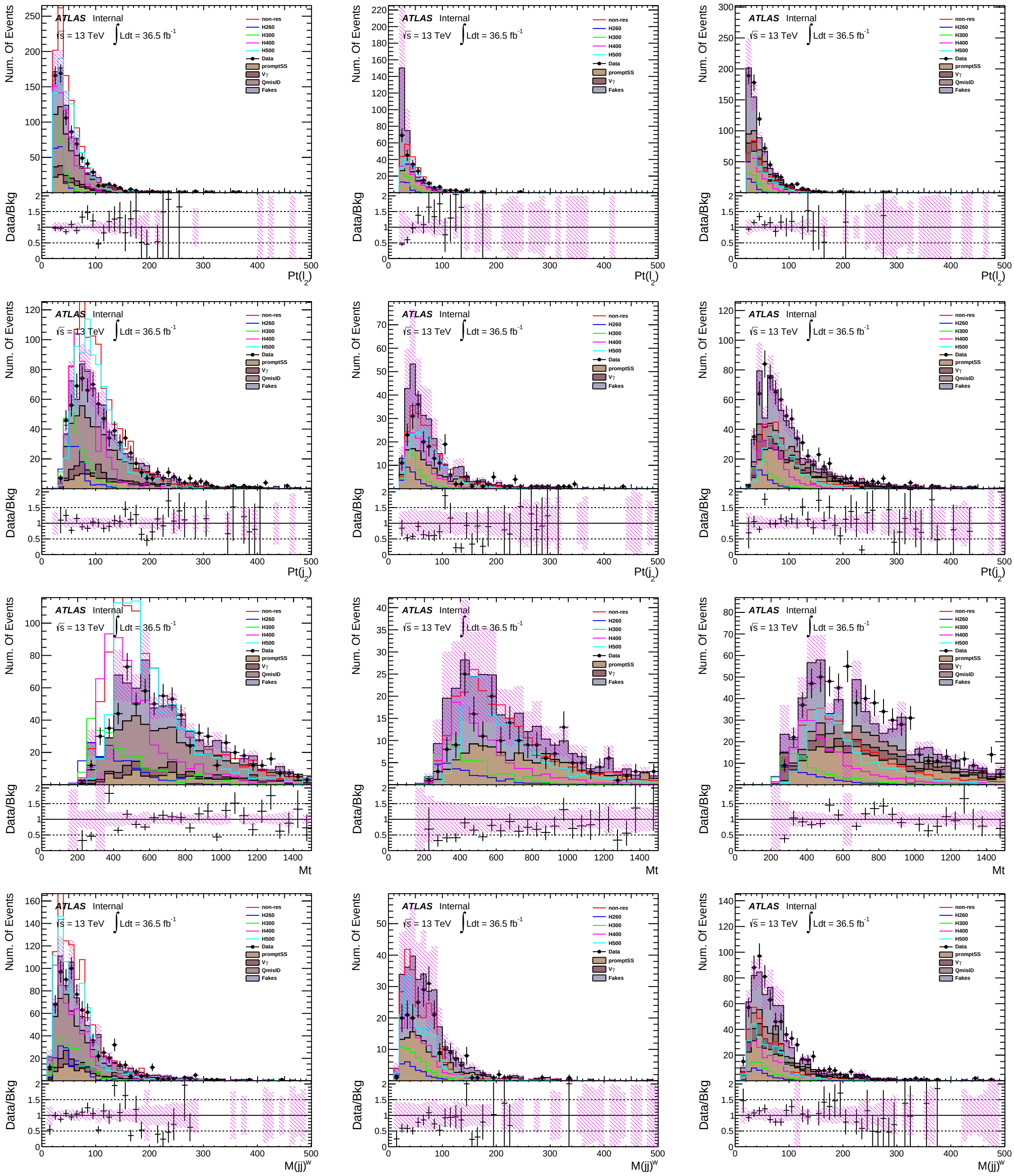

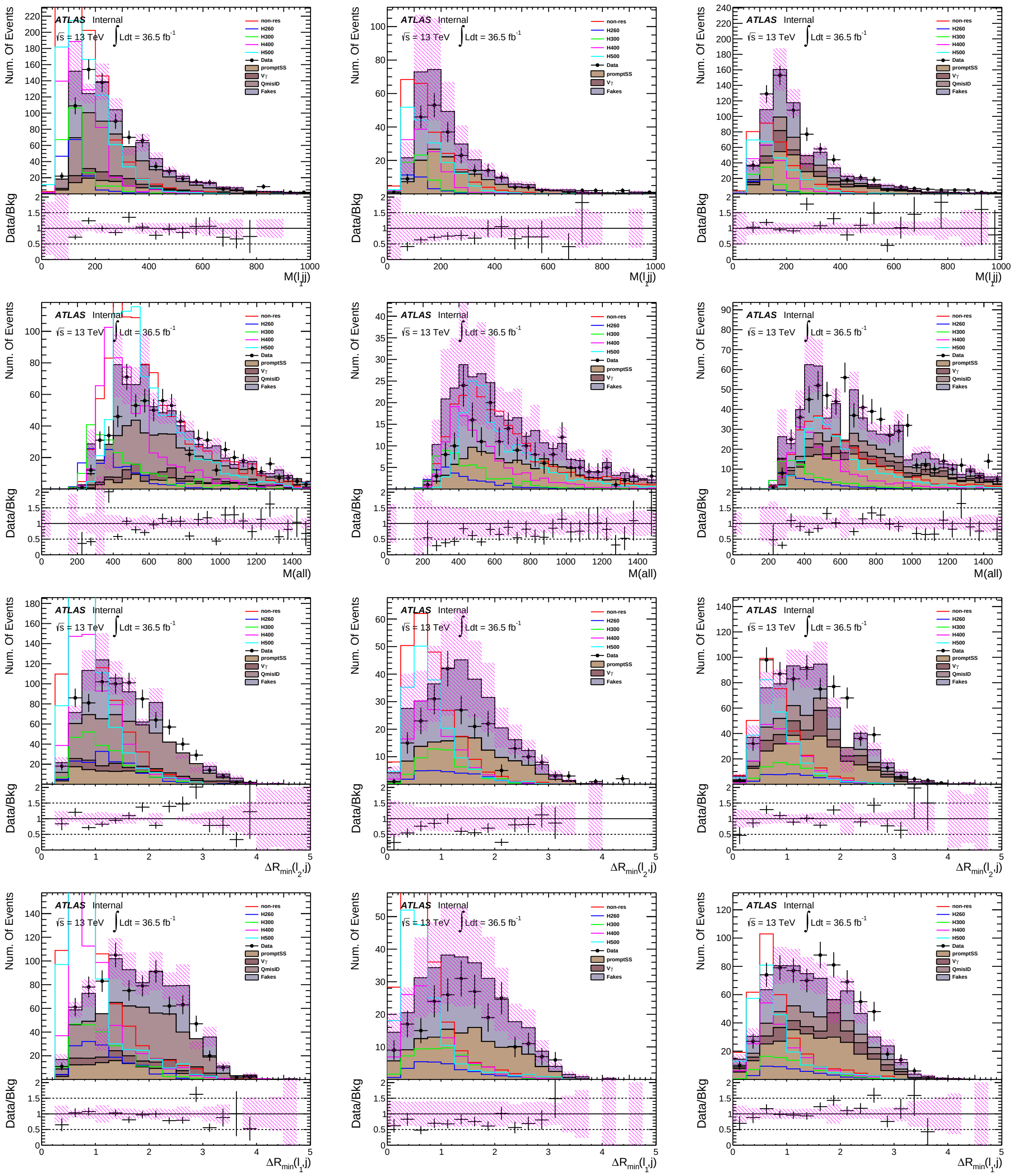

Figure 11: The comparisons between data set and backgrounds in High N_{jet} CR. Left: ee, middle: $e\mu$, right: $e\mu$. The backgrounds consist of promptSS(which contribute two prompt same-sign leptons), QmisID and fakes(jet faking lepton).

Low N_{jet} CR

The comparisons between MC+data-driven backgrounds and data set for various kinematics are made in Low N_{jet} CR. The procedure is similar as what has been described in 5.2.1, but only lower jet multiplicity requirement for all regions. The fake factor is estimated from N_{jet} == 1 region, which then are implemented in N_{jet} >= 2 region. The comparison plots are shown in Fig 12, from which good agreements are observed.

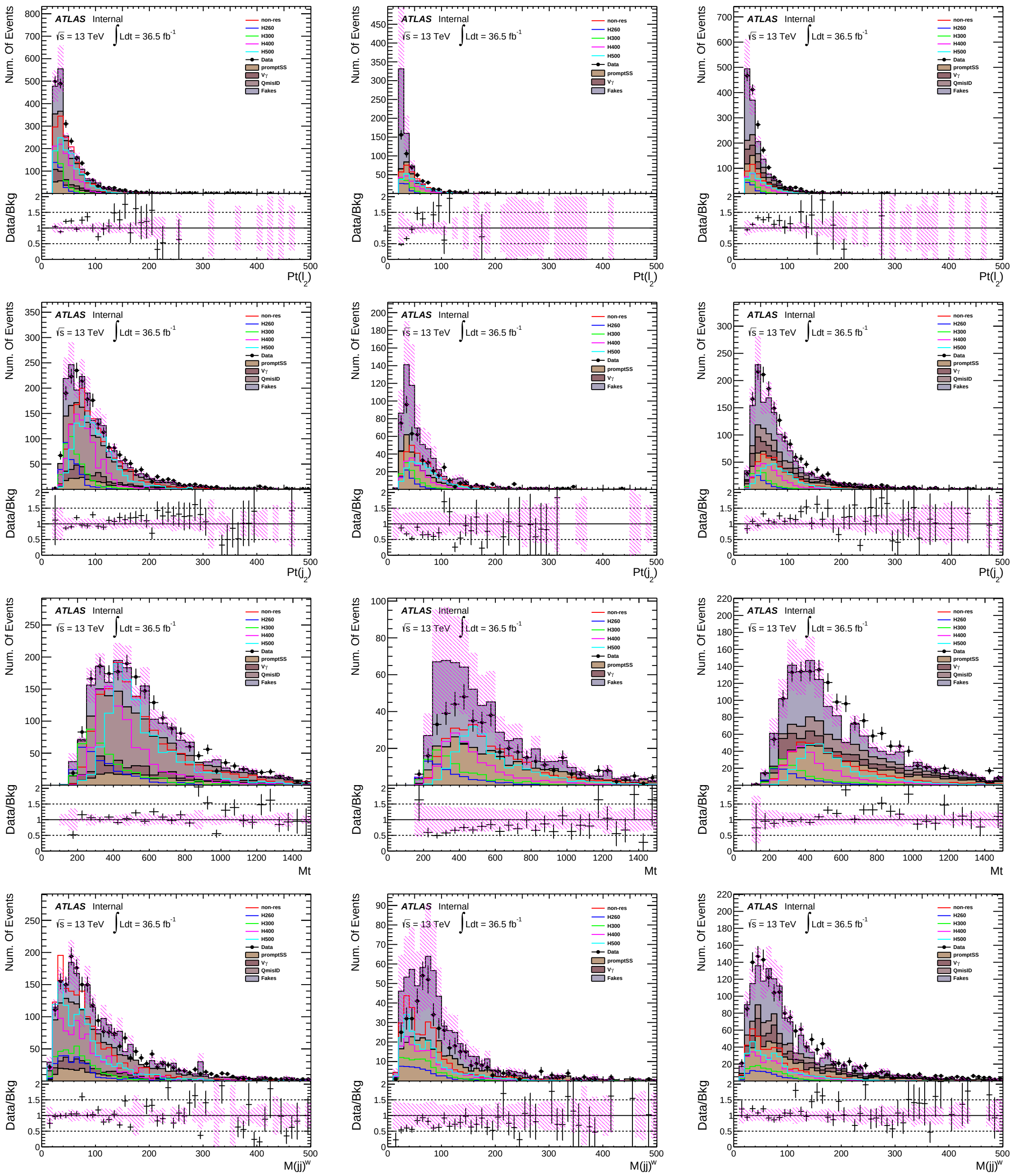

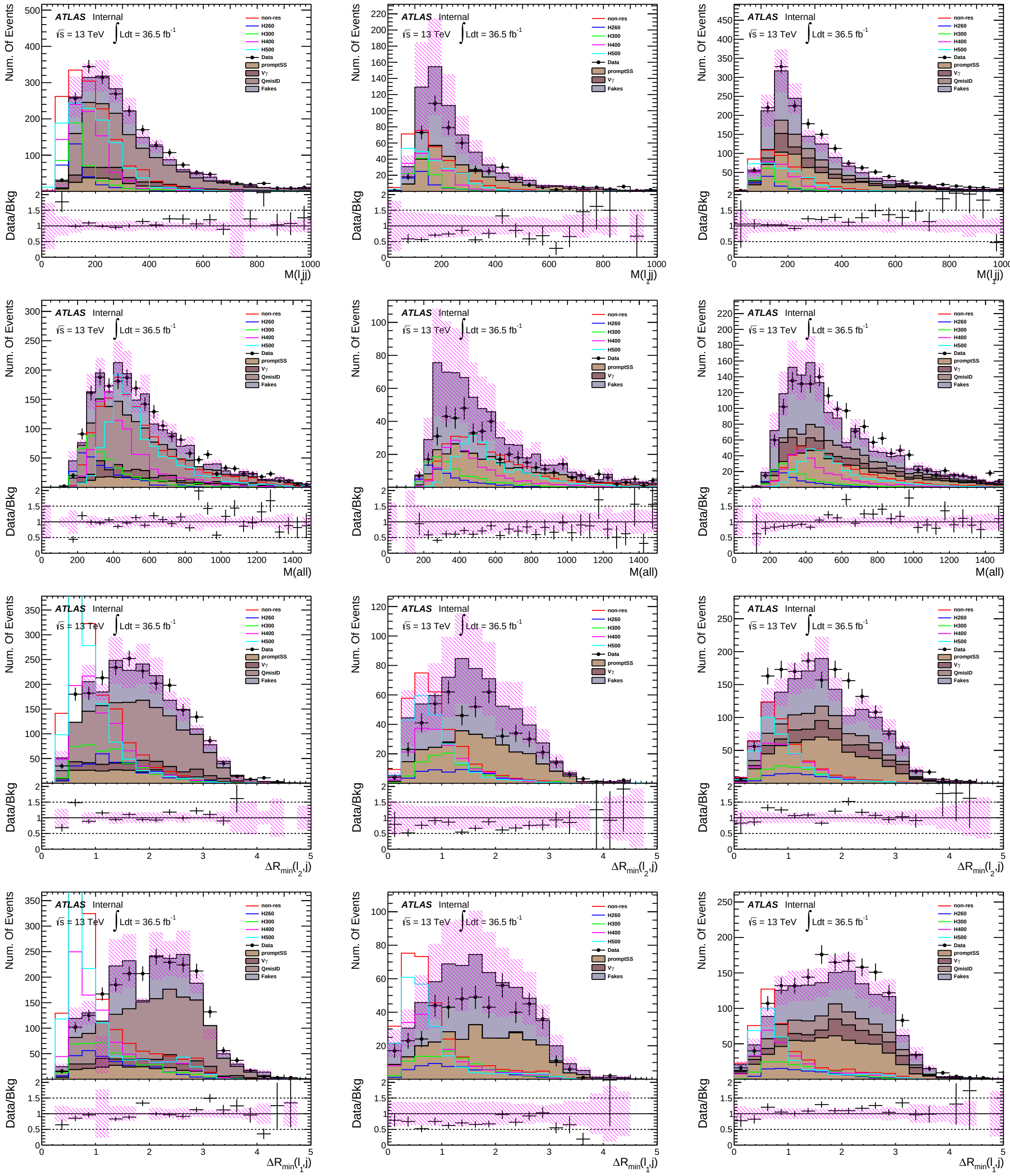

Figure 12: The comparisons between data set and backgrounds in Low N_{jet} CR. Left: ee, middle: $e\mu$, right: $e\mu$. The backgrounds consist of promptSS(which contribute two prompt same-sign leptons), QmisID and fakes(jet faking lepton).

References

[1] ATLAS Collaboration, *Observation of a new particle in the search for the Standard Model Higgs boson with the ATLAS detector at the LHC*, Phys. Lett. B **716** (2012) 1, URL: {http://www.sciencedirect.com/science/article/pii/S037026931200857X}.

[2] CMS Collaboration, *Observation of a new boson at a mass of 125 GeV with the CMS experiment at the LHC*, Phys. Lett. B **716** (2012) 30, URL: {http://www.sciencedirect.com/science/article/pii/S0370269312008581}.

[3] G. Aad et al., *Search For Higgs Boson Pair Production in the $\gamma\gamma b\bar{b}$ Final State using pp Collision Data at $\sqrt{s} = 8$ TeV from the ATLAS Detector*, Phys. Rev. Lett. **114** (2015) 081802, arXiv: 1406.5053 [hep-ex].

[4] G. Aad et al., *Search for Higgs boson pair production in the $b\bar{b}b\bar{b}$ final state from pp collisions at $\sqrt{s} = 8$ TeVwith the ATLAS detector*, Eur. Phys. J. **C75** (2015) 412, arXiv: 1506.00285 [hep-ex].

[5] G. Aad et al., *Searches for Higgs boson pair production in the $hh \to bb\tau\tau, \gamma\gamma WW^*, \gamma\gamma bb, bbbb$ channels with the ATLAS detector*, Phys. Rev. **D92** (2015) 092004, arXiv: 1509.04670 [hep-ex].

[6] U. Baur, T. Plehn and D. Rainwater, *Measuring the Higgs Boson Self-Coupling at the Large Hadron Collider*, Phys. Rev. Lett. **89** (2002) 151801.

[7] L. Qiang and L. Zhao and Q. Yan, and X. Zhao, *Probe Higgs boson pair production via the $3\ell 2j + \overline{)E}$ mode*, Phys. Rev. D **92** (2015) 014015.

[8] ATLAS Collaboration, *Search for the Associated Production of a Higgs Boson and a Top Quark Pair in Multilepton Final States with the ATLAS Detector*, ATLAS-CONF-2016-058, 2016, URL: https://cds.cern.ch/record/2206153.

[9] ATLAS Collaboration, *Evidence of the electroweak production of $W^{\pm}W^{\pm}jj$ in pp collisions at $\sqrt{s} = 8$ TeV with the ATLAS detector*, ATLAS-CONF-2014-013, 2014, URL: https://cds.cern.ch/record/1690282.

[10] ATLAS Collaboration, *The ATLAS Experiment at the CERN Large Hadron Collider*, JINST **3** (2008) S08003.

[11] ATLAS Collaboration, *Performance of the ATLAS Trigger System in 2010*, Eur. Phys. J. C **72** (2012) 1849, arXiv: 1110.1530 [hep-ex].

[12] web pages, F. Maltoni, Higgs pair production. https://cp3.irmp.ucl.ac.be/projects/madgraph/wiki/HiggsPairProduction, Dec 2013.

[13] The ATLAS Collaboration, *Search for heavy neutrino, W_R and Z_R gauge bosons in events with two high-P_T leptons and jets with the ATLAS detector in pp collisions at $\sqrt{s} = 8$ TeV*, ATL-COM-PHYS-2013-810 (2013).

[14] A. Alonso and B. Meirose, *New data-driven methods for lepton charge mis-identification*, ATL-COM-PHYS-2012-164 (2012).

[15] A. L. Read, *Presentation of search results: The CL(s) technique*, J.Phys. **G28** (2002) 2693.

[16] G. Cowan et al., *Asymptotic formulae for likelihood-based tests of new physics*, Eur. Phys. J. **C71** (2011) 1554, arXiv: 1007.1727 [physics.data-an].

List of contributions

Xinchou, Lou	Author's contribution.
Yaquan Fang	Author's contribution.
Weiming Yao	Author's contribution.
Liang Li	Author's contribution.
Xiaohu Sun	Author's contribution.
Shuyang Hu	Author's contribution.
Xingguo Li	Author's contribution.
Maosen Zhou	Author's contribution.

Auxiliary material

In an ATLAS paper, auxiliary plots and tables that are supposed to be made public should be collected in an appendix that has the title ‘Auxiliary material’. This appendix should be printed after the Bibliography. At the end of the paper approval procedure, this information can be split into a separate document – see `atlas-auxmat.tex`.

In an ATLAS note, use the appendices to include all the technical details of your work that are relevant for the ATLAS Collaboration only (e.g. dataset details, software release used). This information should be printed after the Bibliography.